Atmospheric
Chemistry
and Physics

Fine particulate matter in the tropical environment: monsoonal effects, source apportionment, and health risk assessment

M. F. Khan[1,2]**, M. T. Latif**[1,3]**, W. H. Saw**[1]**, N. Amil**[1,4]**, M. S. M. Nadzir**[1,2]**, M. Sahani**[5]**, N. M. Tahir**[6,7]**, and J. X. Chung**[1]

[1]School of Environmental and Natural Resource Sciences, Faculty of Science and Technology, Universiti Kebangsaan Malaysia, 43600 Bangi, Selangor, Malaysia
[2]Centre for Tropical Climate Change System (IKLIM), Institute for Climate Change, Universiti Kebangsaan Malaysia, 43600 Bangi, Selangor, Malaysia
[3]Institute for Environment and Development (LESTARI), Universiti Kebangsaan Malaysia, 43600 Bangi, Selangor, Malaysia
[4]School of Industrial Technology (Environmental Division), Universiti Sains Malaysia, 11800 Penang, Malaysia
[5]Environmental Health and Industrial Safety Program, School of Diagnostic Science and Applied Health, Faculty of Health Sciences, Universiti Kebangsaan Malaysia, Jalan Raja Muda Abdul Aziz, 50300 Kuala Lumpur, Malaysia
[6]Environmental Research Group, School of Marine Science and Environment, Universiti Malaysia Terengganu, 21030 Kuala Terengganu, Terengganu, Malaysia
[7]Institute of Oceanography, Universiti Malaysia Terengganu, 21030 Kuala Terengganu, Terengganu, Malaysia

Correspondence to: M. F. Khan (mdfiroz.khan@ukm.edu.my; mdfiroz.khan@gmail.com)

Abstract. The health implications of $PM_{2.5}$ in the tropical region of Southeast Asia (SEA) are significant as $PM_{2.5}$ can pose serious health concerns. $PM_{2.5}$ concentration and sources here are strongly influenced by changes in the monsoon regime from the south-west quadrant to the north-east quadrant in the region. In this work, $PM_{2.5}$ samples were collected at a semi-urban area using a high-volume air sampler at different seasons on 24 h basis. Analysis of trace elements and water-soluble ions was performed using inductively coupled plasma mass spectroscopy (ICP-MS) and ion chromatography (IC), respectively. Apportionment analysis of $PM_{2.5}$ was carried out using the United States Environmental Protection Agency (US EPA) positive matrix factorization (PMF) 5.0 and a mass closure model. We quantitatively characterized the health risks posed to human populations through the inhalation of selected heavy metals in $PM_{2.5}$. 48 % of the samples collected exceeded the World Health Organization (WHO) 24 h $PM_{2.5}$ guideline but only 19 % of the samples exceeded 24 h US EPA National Ambient Air Quality Standard (NAAQS). The $PM_{2.5}$ concentration was slightly higher during the north-east monsoon compared to south-west monsoon. The main trace metals identified were As, Pb, Cd, Ni, Mn, V, and Cr while the main ions were SO_4^{2-}, NO_3^-, NH_4^+, and Na. The mass closure model identified four major sources of $PM_{2.5}$ that account for 55 % of total mass balance. The four sources are mineral matter (MIN) (35 %), secondary inorganic aerosol (SIA) (11 %), sea salt (SS) (7 %), and trace elements (TE) (2 %). PMF 5.0 elucidated five potential sources: motor vehicle emissions coupled with biomass burning (31 %) were the most dominant, followed by marine/sulfate aerosol (20 %), coal burning (19 %), nitrate aerosol (17 %), and mineral/road dust (13 %). The hazard quotient (HQ) for four selected metals (Pb, As, Cd, and Ni) in $PM_{2.5}$ mass was highest in $PM_{2.5}$ mass from the coal burning source and least in $PM_{2.5}$ mass originating from the mineral/road dust source. The main carcinogenic heavy metal of concern to health at the current location was As; the other heavy metals (Ni, Pb, and Cd) did not pose a significant cancer risk in $PM_{2.5}$ mass concentration. Overall, the associated lifetime cancer risk posed by the exposure of hazardous metals in $PM_{2.5}$ is 3–4 per 1 000 000 people at this location.

1 Introduction

Atmospheric fine particles (PM$_{2.5}$, dP $\leq$ 2.5 µm), a mixture of many inorganic and organic components, reside for a long time in the atmosphere and can penetrate deep into the lungs. Prolonged exposure to PM$_{2.5}$ can cause adverse health impacts and premature mortality in humans (Betha et al., 2014). Potential health benefits and an improvement in general mortality could be expected if the control policies were implemented (Boldo et al., 2011). The adverse effects of PM$_{2.5}$ can reach intercontinental scales (Anenberg et al., 2014) due to the potential transport of PM$_{2.5}$ over hundreds to thousands of kilometres (Seinfeld and Pandis, 2012). The sources of PM$_{2.5}$, particularly motor vehicle emissions, are associated with an increase in hospital admissions (Kioumourtzoglou et al., 2014). A study by Bell et al. (2014) suggested that controlling some of the sources of PM$_{2.5}$ could protect public health more efficiently than the regulation of particle concentration. Thus, the possible reduction in health risks from the predominant sources of PM$_{2.5}$ is desired as part of the mitigation strategy. Diesel emissions and biomass burning, as the primary risk sources of PM$_{2.5}$, should be closely monitored and regulated (Wu et al., 2009).

The identification of PM$_{2.5}$ sources is becoming a widely recognized way to protect human health as well as the environment. Multivariate receptor models are very useful in the source apportionment of PM$_{2.5}$. Widely used multivariate methods are (a) a chemical mass balance model (CMB) (Watson et al., 1990), (b) positive matrix factorization (PMF) (Paatero, 1997; Paatero and Tapper, 1994), (c) Unmix (Henry, 1987), (d) principal component analysis coupled with absolute principal component score (PCA–APCS) (Thurston and Spengler, 1985), (e) pragmatic mass closure (PMC) (Harrison et al., 2003), and (f) a new source-type identification method for PM$_{2.5}$ known as Reduction and Species Clustering Using Episodes (ReSCUE) (Vedantham et al., 2014). PMF is the most reliable method for source-type identification for the following reasons: (i) it uses a weighted least-squares fit and estimates error of the measured data and can impose non-negativity constraints weighing each data point individually (Paatero, 1997; Paatero and Tapper, 1994), (ii) a priori knowledge of pollutants is not necessary, and (iii) it is able to deal with missing values, noisy data, outliers, and values below detection limit (Baumann et al., 2008; Khan et al., 2012, 2015b; Polissar et al., 1998a, b). A recent study by Gibson et al. (2015) suggested that PMF can resolve PM$_{2.5}$ concentrations even below 2 µg m^{-3} more accurately compared to PMC and CMB.

Source apportionment studies of PM$_{2.5}$ based on monsoonal seasonal changes in Malaysia are of widespread interest due to the influence of local sources as well as transboundary haze pollution. This haze pollution reaches its worst level during the south-west (SW) and north-east (NE) monsoons each year. Therefore, the main objectives of this work are to investigate (a) the monsoonal effect on the vari-

ability of PM$_{2.5}$, and its chemical composition, (b) factors influencing the sources of PM$_{2.5}$ and (c) to quantitatively characterize the non-carcinogenic and carcinogenic risks to the potentially exposed human populations by selected heavy metals in PM$_{2.5}$ released from the particular sources. The PM$_{2.5}$ mass concentration contributed by each source will be calculated using PMF 5.0.

2 Methodologies

2.1 Description of the study area

Figure 1 shows the sampling location, which is on the roof top of the Biology Building of the Faculty of Science and Technology (FST), Universiti Kebangsaan Malaysia (UKM), Malaysia (2°55′31.91″ N, 101°46′55.59″ E, about 65 m above sea level). This site is less than 1 km from the main Bangi road.

2.2 Sampling and analysis of PM$_{2.5}$ samples

Sampling was carried out on a 24 h basis for a period from July to September 2013 and January to February 2014 for a total of 27 samples. The PM$_{2.5}$ samples were collected on quartz microfiber filters (203 mm × 254 mm, Whatman™, UK) through a PM$_{2.5}$ high-volume sampler (HVS; Tisch, USA) at a flow rate of 1.13 m^3 min^{-1}. Several other researchers also conducted sampling using the quartz microfiber filters for the analysis of trace metals (H. Li et al., 2015; Martins et al., 2016; Kholdebarin et al., 2015; Cusack et al., 2015; Sánchez-Soberón et al., 2015). Prior to use, the filters were preheated at 500 °C for 3 h to remove any deposited organic compounds. All filter papers either blank or exposed were conditioned in a desiccator for 24 h before and after sampling prior to weighing using a 5-digit high-resolution electronic balance (A&D, GR-202, Japan) with a 0.01 mg detection limit. The filter samples were then stored at −18 °C until the extraction procedure. A microwave-assisted digestion system (Start D, Milestone, Germany) was employed for the preparation of the trace element samples. The microwave was operated at two temperature stages, 180 °C for 20 min and ramping to 220 °C for 15 min. The power was set at 500 watts during the procedure when the number of samples ≤ 3. However, the power was set at 1000 watts if the number of samples exceeded three. A 4 : 1 ratio of 12 mL nitric acid (65 %, Merck KGaA, Germany) and 3 mL hydrogen peroxide (40 %, Merck KGaA, Germany) was used as the reagent in this digestion process. A portion of the filter was soaked in the tetrafluoromethaxil (TFM) vessels (SK-10, Milestone, Germany) of the microwave where total mass of the sample and reagent was maintained below 0.25 g for quality assurance purposes. Upon completion, the samples were filtered using a syringe filter (Acrodisc®, 0.2 µm, Pall Gelman Laboratory, MI, USA) with a 50 cc mL^{-1} Terumo syringe
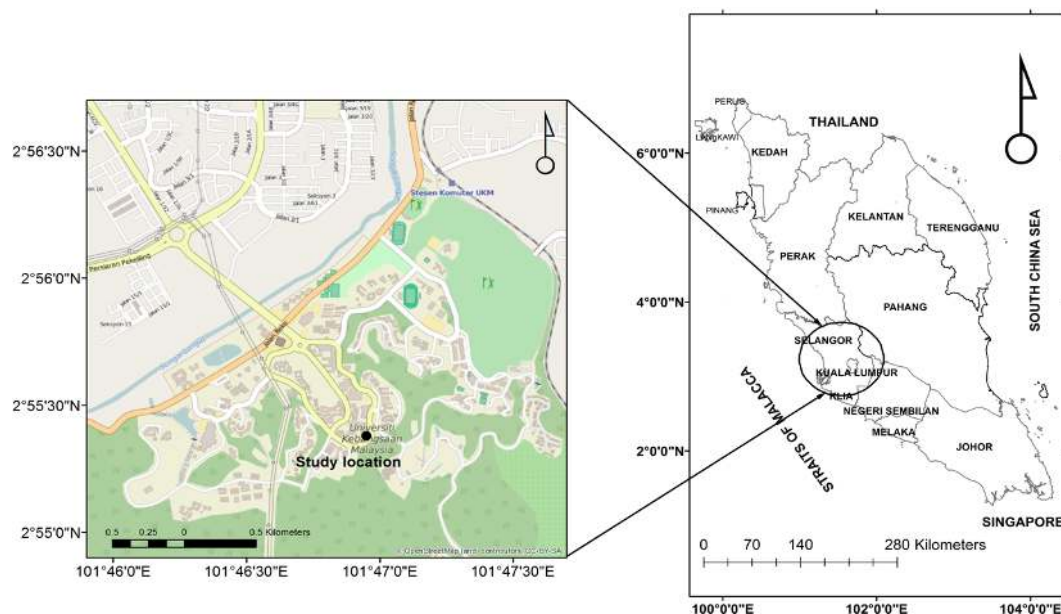
Figure 1. Map of the study area showing the sampling site and nearby line sources.

(Terumo®, Tokyo, Japan) before dilution to 25 mL using ultrapure water (UPW; 18.2 MΩ cm, Easypure® II, Thermo Scientific, Canada). For the preparation of samples for water-soluble ion analysis, a portion of the filter samples was cut into small pieces and placed directly into 50 mL centrifuge tubes with UPW. For this extraction, a combination of ultrasonic vibration, centrifuge, and mechanical shaking were applied. The samples were first sonicated in an ultrasonic bath (Elmasonic S70H, Elma, Germany) for 20 min. Then, the extraction solutions were centrifuged at 2500 rpm (Kubota 5100, Japan) for 10 min before shaken using a vortex mixer for 10 min. The sonication and centrifuged steps were repeated for two more times before the extract was filtered through glass microfiber filters (Whatman™, UK). Both the trace elements and water-soluble ion extracts were refrigerated at 4 °C until further analysis. The trace elements (Al, Ba, Ca, Fe, Mg, Pb, Zn, Ag, As, Cd, Cr, Li, Be, Bi, Co, Cu, Mn, Ni, Rb, Se, Sr, and V) were determined by inductively coupled plasma mass spectroscopy (ICP-MS; PerkinElmer ELAN 9000, USA) while the water-soluble ionic composition (Na$^+$, NH$_4^+$, K$^+$, Ca^{2+}, Mg^{2+}, Cl$^-$, NO$_3^-$, and SO$_4^{2-}$) was determined using ion chromatography (IC) (Metrohm 850 model 881 Compact IC Pro, Switzerland). Metrosep A-Supp 5-150/4.0 and C4-100/4.0 columns were used in the determination of cations and anions, respectively; 1.7 mmol L^{-1} nitric and 0.7 mmol L^{-1} dipicolinic acid (Merck KGaA, Germany) were prepared to be used as eluents for cations. Eluents of 6.4 mmol L^{-1} sodium carbonate (Na$_2$CO$_3$) (Merck KGaA, Germany) and 2.0 mmol L^{-1} sodium bicarbonate (NaHCO$_3$) (Merck KGaA, Germany) were prepared and used to measure anions (Cl$^-$, NO$_3^-$ and

SO$_4^{2-}$) with a flow rate of 0.7 mL min^{-1}; 100 mmol L^{-1} Suprapur® sulfuric acid (H$_2$SO$_4$) (Merck KGaA, Germany) was also prepared to use as a suppressor regenerant and ions were detected by a conductivity detector.

2.3 Quality assurance and quality control

As part of quality assurance and quality control (QA/QC), the concentrations of the composition of PM$_{2.5}$ were corrected from the reagent and filter blanks samples, which were treated with a similar procedure to the exposed filters. To determine the recovery (%) of the heavy metals, a standard reference material (SRM), urban particulate matter SRM 1648a obtained from the National Institute of Standards and Technology (NIST), USA, was treated using the procedures outlined above. The method detection limit (MDL) for trace elements is calculated as 3 times the standard deviation of 10 replicates of the reagent blank. Three samples of filter blanks were used to calculate the MDL of water-soluble ions. Overall MDL were as reported in Table 1. During the trace element analysis by ICP-MS, two modes of analysis were applied with updated calibration curves each time. Based on trial runs and SRM1648a, the elements were initially screened for concentration levels, which resulted in two modes analysis: (a) a set of metals (Al, Ca, Fe, Mg, Zn, and Mn) with high concentrations (with several dilution factors), and (b) a set of metals (Ba, Pb, Ag, As, Cd, Cr, Li, Be, Bi, Co, Cu, Ni, Rb, Se, Sr, and V) with low concentrations.

Table 1. The statistical parameters of the $PM_{2.5}$ and its compositions.

Species	Overall ($n = 27$)		SW[b] ($n = 9$)		NE[c] ($n = 18$)		MDL[d]	Recovery (%)
(ng m^{-3})	Mean ± SD[a]	Range	Mean ± SD	Range	Mean ± SD	Range		
Al	267.6 ± 145.0	98.48–826.6	203.1 ± 118.42	98.48–416.09	299.8 ± 149.2	101.9–826.6	0.70	70 (54–97)
Ba	1660 ± 1501	319.2–6092	1372 ± 1480	319.2–5187	1804 ± 1532	447.6–6092	0.02	–
Ca	1770 ± 725.9	n.d.–3150	1584 ± 325.5	1234–2154	1975 ± 683.4	882.1–3150	2.88	33 (23–47)
Fe	3052 ± 654.6	2171–4567	2513 ± 239.6	2171–2893	3322 ± 630.4	2530–4567	0.40	80 (69–95)
Mg	207.6 ± 83.85	34.43–371.7	207.1 ± 72.85	119.0–356.0	207.9 ± 90.86	34.43–371.7	0.17	95 (81–111)
Pb	21.84 ± 16.30	3.57–76.17	28.06 ± 20.27	13.1–76.17	18.72 ± 13.49	3.57–51.70	0.01	119 (89–134)
Zn	389.2 ± 179.8	178.8–817.9	526.8 ± 236.3	178.8–817.9	320.4 ± 90.25	184.7–448.2	0.22	102 (84–129)
Ag	0.09 ± 0.05	n.d.–0.21	0.05 ± 0.04	0.01–0.11	0.10 ± 0.05	0.02–0.21	0.01	120 (97–170)
As	5.76 ± 4.74	1.10–18.33	5.22 ± 2.93	1.55–9.79	6.04 ± 5.49	1.10–18.33	0.45	88 (81–94)
Cd	0.54 ± 0.29	0.13–1.15	0.44 ± 0.22	0.13–0.81	0.58 ± 0.32	0.17–1.15	< 0.01	85 (81–89)
Cr	107.68 ± 18.57	82.32–152.62	91.06 ± 7.52	82.32–104.4	115.9 ± 16.78	91.17–152.6	0.02	56 (31–87)
Li	0.22 ± 0.12	0.04–0.43	0.11 ± 0.06	0.04–0.21	0.28 ± 0.10	0.07–0.43	0.09	–
Be	0.01 ± 0.01	n.d.–0.03	0.003 ± 0.01	n.d.–0.01	0.01 ± 0.01	n.d.–0.03	< 0.01	–
Bi	0.76 ± 0.60	0.08–2.08	0.67 ± 0.35	0.13–1.17	0.80 ± 0.70	0.08–2.08	0.03	–
Co	0.85 ± 0.47	0.39–2.36	1.16 ± 0.61	0.39–2.36	0.70 ± 0.30	0.39–1.38	0.08	96 (87–109)
Cu	28.33 ± 11.02	16.83–62.55	32.39 ± 10.08	19.78–49.27	26.30 ± 11.17	16.83–62.55	0.30	101 (96–105)
Mn	4.03 ± 1.91	0.23–7.18	3.13 ± 2.07	0.23–6.08	4.49 ± 1.71	1.46–7.18	0.95	126 (114–147)
Ni	17.24 ± 8.55	7.86–46.70	23.59 ± 11.11	7.86–46.70	14.06 ± 4.66	8.84–27.03	0.67	91 (82–99)
Rb	3.59 ± 1.08	1.74–6.16	4.14 ± 1.29	2.23–6.16	3.32 ± 0.87	1.74–4.69	0.13	78 (52–113)
Se	0.65 ± 0.33	0.20–1.24	0.36 ± 0.10	0.20–0.53	0.79 ± 0.31	0.39–1.24	0.09	94 (78–110)
Sr	40.25 ± 31.05	13.75–120.93	35.88 ± 32.10	13.75–118.47	42.43 ± 31.22	15.72–120.9	0.38	91 (75–125)
V	5.13 ± 3.05	0.63–13.16	3.70 ± 2.47	0.63–7.82	5.85 ± 3.12	2.21–13.16	< 0.01	85 (77–93)
Na$^+$	532.1 ± 262.0	n.d.–1029.07	363.9 ± 185.6	159.9–778.8	606.90	23.66–1029.1	62.68	–
NH$_4^+$	598.9 ± 399.2	82.60–1622.17	542.5 ± 320.8	82.60–1141.4	627.2 ± 439.0	105.5–1622.2	–	–
K$^+$	343.3 ± 183.2	70.18–696.04	307.8 ± 103.5	175.6–484.6	361.1 ± 212.7	70.18–696.0	2.35	–
Ca^{2+}	255.9 ± 84.22	87.55–455.55	295.1 ± 95.8	186.4–455.6	236.3 ± 72.84	87.55–360.4	23.21	–
Mg^{2+}	42.26 ± 17.57	12.70–77.60	32.61 ± 18.32	12.70–71.94	47.09 ± 15.49	15.65–77.60	23.71	–
Cl$^-$	56.71 ± 44.94	4.67–151.18	67.63 ± 24.21	40.07–107.18	51.25 ± 52.13	4.67–151.2	0.98	–
NO$_3^-$	926.9 ± 1031.8	98.66–3523.7	194.8 ± 73.63	98.66–311.3	1293 ± 1095	136.5–3524	16.51	–
SO$_4^{2+}$	2127 ± 2068	n.d.–6211	n.d.	n.d.	2127 ± 2068	350.5–6211	1.82	–
PM$_{2.5}^e$	25.13 ± 9.21	7.01–42.28	22.16 ± 9.14	7.01–35.73	26.61 ± 9.14	12.76–42.28	–	–

[a] SD: standard deviation; [b] SW: south-west monsoon; [c] NE: north-east monsoon; [d] MDL: method detection limit; [e] $PM_{2.5}$ (µg m^{-3}); n.d.: not detected; "–": no data.

2.4 Local circulation of wind and biomass fire hotspots

Each year, Peninsular Malaysia experiences two monsoon regimes, the SW monsoon (June–September) and the NE monsoon (December–March). During the SW monsoon, south-west winds dominate the wind pattern in Peninsular Malaysia, inducing drier weather. During the NE monsoon, strong north-east winds dominate over Peninsular Malaysia, bringing more rainfall to the east coast. To investigate this, the regional synoptic wind field 10 m above the surface and a resolution of $0.25 \times 0.25°$ ranging from $-10°$ S to 25° N, 85 to 125° E was plotted using open Grid Analysis and Display System (GrADS version 2.0.2). The wind field used to demonstrate the monsoon regimes in this study is a gridded product produced by the global atmospheric reanalysis known as ERA-Interim, by the European Centre for Medium-Range Weather Forecasts (ECMWF) (Dee et al., 2011).

The ERA-Interim 10 m surface wind vectors (January 2004 to June 2014) show the two opposite monsoon regimes experienced by Peninsular Malaysia (Fig. 2). It can be seen that the south-west wind, from June to August, that blew from Sumatra Island, Indonesia, to Peninsular Malaysia was generally weaker with wind speed around 1–2 m s^{-1}. Whereas the north-east wind, from November to January, was much stronger, with wind speeds of around 5–7 m s^{-1} (Fig. 2).

Biomass fire hotspots and the travel path of the monthly back trajectories of each season were also plotted (Fig. 3). The mean clusters of back trajectories were produced using the Hybrid Single-Particle Lagrangian Integrated Trajectory Model (HYSPLIT 4.9), and were re-plotted using the graphical software, IGOR Pro 6.0.1 (WaveMetrics, OR, USA). A release height of about 500 m for 120 h back trajectories with 6 h intervals was chosen. Trajectory start time was chosen at 16:00 (UTC) to represent 24:00 (local time). The cluster mean of trajectories was regarded by numeral number and colour (1 – red, 2 – green, 3 – turquoise, and 4 – purple). The fire hotspot data of the Moderate Resolution Imaging Spectroradiometer (MODIS) were used to investigate the biomass burning hotspots in the specific area of interest. The data were downloaded from the National Aeronautics and Space Administration (NASA) Land Atmo-
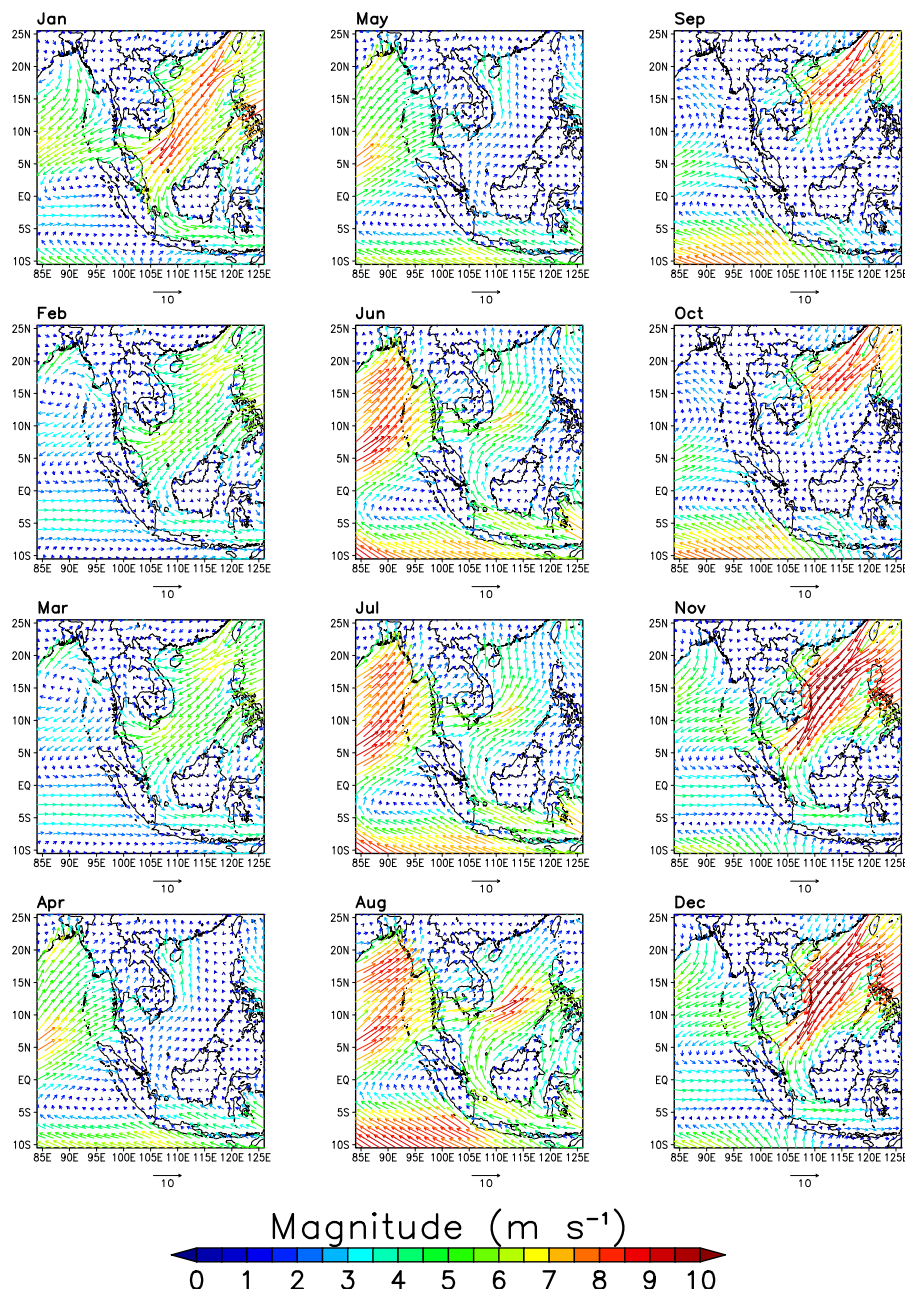
Figure 2. Monthly climatology wind vector from January 2004 to June 2014.

sphere near-Real-Time Capability for Earth Observing System (EOS) Fire Information for Resource Management System (NASA LANCE FIRMS) fire archive covering an area from 15° S to 30° N and 80° W to 130° E. In addition, to investigate the variability of the boundary layer height around the region of Peninsular Malaysia, ERA-Interim boundary layer height (BLH) gridded data from January 2000 to December 2014 were downloaded from the ECMWF. The resolution of this data was 0.5° × 0.5°, covering the domain of Peninsular Malaysia (99–105° E, 0–9° N). Yearly daily means of the ERA-Interim BLH data were calculated us-

ing the climate data operators (CDO) version 1.6.9 software (https://code.zmaw.de/projects/cdo) developed by the Max Plank Institute, by first calculating the area mean.

2.5 Enrichment factor

The enrichment factor (EF) of the heavy metals was calculated based on the abundance of elements in the Earth's crust published by Taylor (1964). The EF of each element can be defined using the following equation
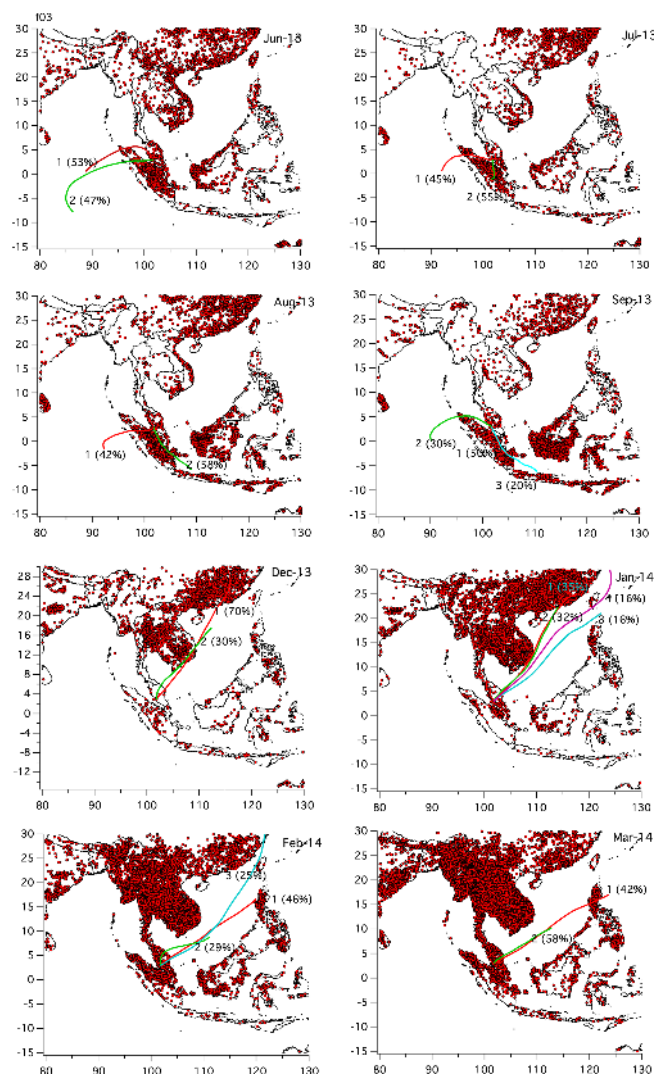
Figure 3. The location of biomass fire hotspots and the monthly mean cluster of backward trajectories by HYSPLIT 4.9 model for 120 h and 500 m releasing height starting from 16:00 UTC during the south-west and the north-east monsoon.

$$EF = \frac{\left(\frac{E}{Al}\right)_{PM_{2.5}}}{\left(\frac{E}{Al}\right)_{Crust}}, \quad (1)$$

where E / Al is the concentration ratio of element, E, to the reference metal, Al. Al was selected as the reference element to calculate the annual and seasonal EF. Several other researchers also used Al as the reference element (Birmili et al., 2006; Khan et al., 2010a; Sun et al., 2006). Chester et al. (2000), Cheung et al. (2012), Khan et al. (2010a), Mohd Tahir et al. (2013), and Torfs and Van Grieken (1997) proposed a EF cut-off of 10 to differentiate between crustal and natural and anthropogenic origins of heavy metals. Thus, we consider EF = 10 as the cut-off point. Therefore, a good number of the metals (Zn, Cr, Rb, Be, V, Fe, Ca, Co, Sr, Pb, As,

and Bi) in $PM_{2.5}$ in this study can be assumed to originate from anthropogenic sources (Fig. 5a). These heavy metals were not natural or from the Earth's crust. No seasonal differences were observed in the EF of the heavy metals.

2.6 Mass closure model

A study by Harrison et al. (2003) introduced a PMC model for the source apportionment of particulate matter, which is the basis for this study. The variables were grouped into the following four sub-classes: (i) mineral matter (MIN), (ii) sea salts (SS), (iii) secondary inorganic aerosol (SIA), (iv) trace elements (TE), and (v) undefined (UD). MIN is derived from the sum of Al, Mg, K, Ca, and Fe multiplied by the appropriate factors to convert them into their corresponding oxides as described by the following Eq. (2). Ca was multiplied by a factor of 1.95 to account for CaO and $CaCO_3$ as this metal is assumed to be present in these two forms (Remoundaki et al., 2013; Sillanpää et al., 2006; Terzi et al., 2010)

$$MIN = 1.89\,Al + 1.66\,Mg + 1.21\,K + 1.95\,Ca + 1.43\,Fe. \quad (2)$$

The contribution of SS was estimated by assuming that soluble Na^+ in $PM_{2.5}$ samples originated solely from the marine source and is based on the composition of seawater, ignoring potential atmospheric transformation (Seinfeld and Pandis, 2012). Following Terzi et al. (2010), the composition of sea salt comprised of the following Eq. (3)

$$SS = [Na^+] + [ss\text{-}Cl^-] + [ss\text{-}Mg^{2+}] + [ss\text{-}K^+]$$
$$+ [ss\text{-}Ca^{2+}] + [ss\text{-}SO_4^{2-}], \quad (3)$$

where $ss\text{-}Cl^- = 1.8{*}Na^+$, $ss\text{-}Mg^{2+} = 0.12{*}Na^+$, $ss\text{-}K^+ = 0.036{*}Na^+$, $ss\text{-}Ca^{2+} = 0.038{*}Na^+$, and $ss\text{-}SO_4^{2-} = 0.252{*}Na^+$. Meanwhile, SIA can be estimated by the sum of non-sea-salt sulfate ($nss\text{-}SO_4^{2-}$), NO_3^- and NH_4^+ as explained by Remoundaki et al. (2013) and Terzi et al. (2010) with the following Eq. (4)

$$SIA = [nss\text{-}SO_4^{2-}] + [NO_3^-] + [NH_4^+]. \quad (4)$$

Finally, TE is calculated by the sum of rest of the metals analysed in this study and UD represents unidentified gravimetric mass of $PM_{2.5}$. Therefore, the overall mass closure equation applied in this work can be expressed as the following Eq. (5)

$$PM_{2.5}\,MC = MIN\,(1.89\,Al + 1.66\,Mg + 1.21\,K + 1.95\,Ca$$
$$+ 1.43\,Fe) + SS\,([Na^+] + [ss\text{-}Cl^-] + [ss\text{-}Mg^{2+}]$$
$$+ [ss\text{-}K^+] + [ss\text{-}Ca^{2+}] + [ss\text{-}SO_4^{2-}])$$
$$+ SIA\,([nss\text{-}SO_4^{2-}] + [NO_3^-] + [NH_4^+])$$
$$+ TE + UD. \quad (5)$$

2.7 Source apportionment of PM$_{2.5}$ using PMF

Source apportionment of PM$_{2.5}$ was conducted using the US EPA PMF 5.0 model of the United States Environmental Protection Agency (US EPA) as suggested by Norris et al. (2014). The PMF model is a mathematical factor-based receptor model that interprets source types with a robust uncertainty estimate. Two sets of data were run through the PMF model: (i) concentration and (ii) uncertainty. The concentration of each element was pretreated and validated based on the outliers, missing values and/or values below MDL. In particular, variables with outliers were excluded. Species with concentrations below MDL were replaced with the half of the MDL (Baumann et al., 2008; Polissar et al., 1998a, b). The uncertainty value of each variable of each sample was calculated following the empirical formula Eq. (6)

$$\sigma_{ij} = 0.01 \left(X_{ij} + \overline{X_j} \right), \tag{6}$$

where σ_{ij} is the estimated measurement error for jth species in the ith sample, X_{ij} is the observed elements concentration, and $\overline{X_j}$ is the mean value. The factor 0.01 was determined through trial and error procedures following by Ogulei et al. (2006a). Thus, the measurement of uncertainty (S_{ij}) can be computed with Eq. (7) as applied by Chueinta et al. (2000):

$$S_{ij} = \sigma_{ij} + C X_{ij}, \tag{7}$$

where σ_{ij} the estimation of measurement error (Eq. 6) and C is a constant. In this study, we used a value of 0.4 for C, which, according to Ogulei et al. (2006b), produced the best Q value as it is the closest to theoretical value and physically interpretable results. Other main researchers have also applied this procedure for the calculation of uncertainty (Harrison et al., 2011; Hedberg et al., 2005; Khan et al., 2015b). An additional 5 % uncertainty was added to cover any methodological errors during the preparation of filter papers, gravimetric mass measurements, and preparing the calibration curves.

Initially, PMF factors were resolved using the numbers of 20 runs with a seed value of 9. The number of factors was changed to optimize the goodness-of-fit parameter of Q over the theoretical Q. Five factors were decided upon based on the lowest Q (Robust) and Q (True) value of 180.26 with the Q (true) $/Q_{exp}$ value of 0.50 after 604 computational steps and the convergence of the PMF results. The Q/Q_{exp} ratio for most of the variables was < 5 to 0.92,, which indicates that the Q values were very similar to the expected value. Some of the variables, however, showed a ratio of 0.5 because the computed Q values were smaller than the expected Q values. A study by Brown et al. (2012) described this discrepancy as contributing to the increase of global uncertainty. However, the sharp drop for PM$_{2.5}$ mass ratio (0.03) was due to the down-weighting of the signal to noise (S/N) values. To show the stability of the results, we estimated the error of the con-centration for each variable using bootstrap (BS), displacement (DISP), and a combination of BS-DISP. A comparison of the error estimates with base model runs is demonstrated in Fig. S1 in the Supplement. The five-factor results were relatively stable with meaningful physical interpretation and satisfactorily comparable with the bootstrap analysis. Fe and Cr were reported as outliers and therefore excluded in the calculation. Referring to Table 2, the overall PM$_{2.5}$ concentration is well explained within ± 10 % by the PMF 5.0 considering the $f_{peak} = 0$.

2.8 Health risk assessment of PM$_{2.5}$ and associated various sources

The human health risk posed by heavy metals may occur through inhalation of PM$_{2.5}$. We applied the US EPA supplemented guidance to estimate the risk posed by heavy metals in PM$_{2.5}$ mass concentration and their various sources. As part of the health risk assessment (HRA), we considered lifetime non-carcinogenic and carcinogenic risk. US EPA (2011) describes the exposure concentration for inhalation (EC$_{inh}$) by the following equation

$$EC_{inh} = C \times \frac{ET \times EF \times ED}{ATn}, \tag{8}$$

where C is the concentration of metals in PM$_{2.5}$ estimated for each source with $\mu g\, m^{-3}$ unit for the estimation of EC$_{inh}$; EF is the exposure frequency (151 days year^{-1}) representing July, August, September, January, and February; ED is exposure duration (24 years for adult); BW is the average body weight (70 kg for adult); ET is the exposure time (h day^{-1}); and ATn is the average time (ATn $=$ ED $\times$ 365 days $\times$ 24 h day^{-1} for non-carcinogenic and ATn $=$ 70 year $\times$ 365 days year^{-1} $\times$ 24 h day^{-1} for carcinogenic risk). ED, BW, and AT values are based on the study by Hu et al. (2012).

Further, we examined the non-carcinogenic risk (presented by the hazard quotient, HQ) and lifetime carcinogenic risk (LCR) of selected heavy metals as classified by the International Agency for Research on Cancer (IARC). The following equations were involved for the calculation of HQ and LCR:

$$HQ = \frac{EC_{inh}}{\left(RfC_i \times 1000\,\mu g\, m^{-3} \right)} \tag{9}$$

$$LCR = IUR \times EC_{inh}, \tag{10}$$

where RfC_i is the inhalation reference concentration (mg m^{-3}), and IUR is the inhalation unit risk ((µg m^{-3})$^{-1}$). The non-carcinogenic risk or HQ represents the observable health effects from exposure to the PM$_{2.5}$ based on the dose–response relationship principles. The cut-off point for significant health risks to the exposed population is HQ > 1. The carcinogenic risk refers to a person's chance of developing cancer from exposure to any carcinogenic

Table 2. The contribution of sources to $PM_{2.5}$ and the compositions estimated by PMF 5.0 model.

Variables	Mineral/road dust (mean ± SD[a])		Motor vehicle emissions/ biomass burning (mean ± SD)		Nitrate aerosol (mean ± SD)		Coal burning (mean ± SD)		Marine/sulfate aerosol (mean ± SD)	
	ng m⁻³	%	ng m⁻³	%	ng m⁻³	%	ng m⁻³	%	ng m⁻³	%
$PM_{2.5}$	3.17 ± 0.15[b]	13 ± 1	7.47 ± 1.26[b]	31 ± 5	4.11 ± 0.47[b]	17 ± 2	4.60 ± 0.37[b]	19 ± 2	4.99 ± 0.67[b]	20 ± 3
Al	42.65 ± 3.17	19 ± 1	45.37 ± 3.85	20 ± 2	69.06 ± 2.45	31 ± 1	29.84 ± 1.73	13 ± 1	36.71 ± 2.51	16 ± 1
Ba	269.3 ± 205.9	22 ± 17	32.85 ± 146.9	3 ± 14	166.9 ± 71.90	13 ± 6	661.7 ± 246.9	52 ± 19	117.8 ± 116.8	10 ± 11
Ca	445.1 ± 32.07	28 ± 2	235.43 ± 37.76	15 ± 2	350.6 ± 35.82	22 ± 2	303.4 ± 30.14	19 ± 2	267.1 ± 26.00	17 ± 2
Mg	92.36 ± 5.02	52 ± 3	47.59 ± 21.66	27 ± 12	25.43 ± 12.33	14 ± 7	10.32 ± 6.11	6 ± 3	1.23 ± 5.50	1 ± 3
Pb	3.56 ± 0.79	20 ± 4	9.11 ± 2.32	50 ± 13	0.58 ± 0.40	3 ± 2	3.61 ± 0.42	20 ± 2	1.25 ± 1.36	7 ± 8
Zn	157.7 ± 17.09	48 ± 5	45.66 ± 30.11	14 ± 9	60.74 ± 21.74	18 ± 7	50.56 ± 19.46	15 ± 6	14.33 ± 8.53	4 ± 3
As	0.18 ± .35	4 ± 7	1.76 ± 0.55	41 ± 14	0.05 ± 0.10	1 ± 2	2.37 ± 0.65	53 ± 13	0.05 ± 0.22	1 ± 6
Cd	0.03 ± 0.01	6 ± 2	0.22 ± 0.06	44 ± 12	0.07 ± 0.02	13 ± 3	0.13 ± 0.02	27 ± 3	0.05 ± 0.02	10 ± 5
Cu	12.38 ± 0.59	50 ± 2	3.55 ± 2.37	14 ± 10	4.20 ± 1.45	17 ± 6	3.27 ± 1.16	13 ± 5	1.45 ± 0.42	6 ± 2
Mn	–	–	0.84 ± 0.27	25 ± 8	1.16 ± 0.19	35 ± 6	0.62 ± 0.26	18 ± 7	0.71 ± 0.09	21 ± 3
Ni	7.21 ± 0.50	48 ± 4	2.79 ± 1.18	18 ± 8	1.70 ± 0.77	11 ± 5	3.11 ± 0.80	20 ± 5	0.36 ± 0.23	2 ± 2
Rb	1.33 ± 0.07	38 ± 2	0.76 ± 0.20	22 ± 6	0.45 ± 0.14	13 ± 4	0.67 ± 0.10	19 ± 3	0.26 ± 0.04	7 ± 1
Se	0.05 ± 0.01	8 ± 2	0.14 ± 0.03	24 ± 6	0.14 ± 0.02	23 ± 3	0.11 ± 0.02	19 ± 3	0.16 ± 0.01	27 ± 1
Sr	8.26 ± 4.51	25 ± 14	1.19 ± 3.18	4 ± 11	4.60 ± 1.80	14 ± 6	15.05 ± 5.05	45 ± 15	3.59 ± 2.40	11 ± 9
V	0.19 ± 0.08	5 ± 2	0.81 ± 0.24	20 ± 6	1.25 ± 0.20	30 ± 6	0.59 ± 0.32	14 ± 7	1.28 ± 0.17	31 ± 4
Na^+	88.10 ± 28.60	19 ± 6	17.28 ± 56.76	4 ± 12	120.8 ± 10.99	26 ± 3	7.93 ± 4.69	2 ± 1	234.2 ± 20.31	50 ± 5
NH_4^+	59.48 ± 30.60	11 ± 6	241.1 ± 61.51	44 ± 11	82.56 ± 18.67	15 ± 4	8.55 ± 16.10	2 ± 3	156.2 ± 48.24	28 ± 8
K^+	65.10 ± 18.20	20 ± 6	91.08 ± 16.94	28 ± 5	50.69 ± 6.14	16 ± 2	9.53 ± 3.42	3 ± 1	108.4 ± 16.41	33 ± 5
Ca^{2+}	99.79 ± 3.69	42 ± 1	50.52 ± 18.74	21 ± 8	47.25 ± 9.79	20 ± 4	12.39 ± 6.67	5 ± 3	26.39 ± 4.03	11 ± 2
Mg^{2+}	8.18 ± 1.46	23 ± 4	6.96 ± 1.06	19 ± 3	9.27 ± 0.31	26 ± 1	1.92 ± 0.38	5 ± 1	9.72 ± 0.32	27 ± 1
Cl^-	15.88 ± 4.06	36 ± 10	1.83 ± 2.95	4 ± 8	–	–	5.90 ± 0.73	13 ± 2	20.58 ± 6.45	46 ± 13
NO_3^-	90.86 ± 36.16	11 ± 4	6.66 ± 21.39	1 ± 2	611.0 ± 27.43	75 ± 3	5.75 ± 16.39	1 ± 2	103.4 ± 53.25	13 ± 7
SO_4^{2-}	307.2 ± 142.1	21 ± 10	58.02 ± 152.1	4 ± 11	74.23 ± 33.91	5 ± 2	89.77 ± 10.15	6 ± 1	935.1 ± 112.5	64 ± 7

[a] SD: standard deviation; [b] unit: µg m⁻³; "–": no data.

agent. LCR represents the excess lifetime cancer risk described in terms of the probability that an exposed individual will develop cancer because of that exposure by age 70 as defined by US EPA Risk Communication (http://www.epa.gov/superfund/community/pdfs/toolkit/ risk_communicati-onattachment6.pdf). The carcinogenic risk from the lifetime exposure of those hazardous metals is regulated by the acceptable or tolerance level (1×10^{-6}) set by the US EPA, which corresponds to lifetime exposure to an unpolluted environment (Satsangi et al., 2014).

3 Results and discussions

3.1 Concentration of $PM_{2.5}$ and its chemical composition

Table 1 summarizes the statistics from the SW monsoon, the NE monsoon and overall concentrations of $PM_{2.5}$, heavy metals and major ions. Overall, the 24 h average values of $PM_{2.5}$ (avg = 25.13 µg m⁻³) in the study area are slightly higher than that of the WHO 24 h guideline (25 µg m⁻³) but lower than that of 24 h US EPA National Ambient Air Quality Standard (NAAQS) (35 µg m⁻³). Of the samples taken during the day, 48 % exceeded the WHO 24 h guideline while 19 % of them exceeded the US EPA 24 h NAAQS for $PM_{2.5}$ (currently, Malaysia has no set guidelines for $PM_{2.5}$). If we compare the $PM_{2.5}$ overall value of 25.13 µg m⁻³ with

the yearly mean of US EPA NAAQS (15 µg m⁻³), WHO (10 µg m⁻³), European Union (EU) (25 µg m⁻³), or Department of Environment (DoE) (Australia) (8 µg m⁻³), the concentration of $PM_{2.5}$ is much higher with respect the guideline set by all regulatory bodies. The average value of $PM_{2.5}$ during the NE monsoon was slightly higher than the SW monsoon. During the south-west monsoon season, $PM_{2.5}$ was mainly carried by the prevailing south-west wind from the Sumatra Island of Indonesia, which is located at the south-west quadrant of the Southeast Asia (SEA) region. On the other hand, during the north-east monsoon season, the $PM_{2.5}$ sources can be traced back to the Chinese mainland, Indochina region, and the Philippines. This is due to the prevailing north-east wind transporting $PM_{2.5}$ from these locations to the tropical region of SEA. The Student t test for paired independent samples showed that the mean during these two monsoons varies insignificantly ($t = 1.19$, $p > 0.05$). However, the monsoonal changes in this region as displayed in Fig. 3, showed that air masses of different origins transport different pollutants to the area. The back trajectory plots showed that there were high numbers of biomass fire hotspots during both seasons but from different regions (Fig. 3). The period of June to September is the dry season each year in Malaysia and Sumatra of Indonesia. During this dry season, biomass fire hotspots are densely located in this area due to the burning of agricultural waste and forest fires. Several other researchers also reported the high number

of biomass fire-related hotspots to these regions (Khan et al., 2015c; Sahani et al., 2014).

On the other hand, December to March is usually the wet season in Malaysia. However, the backward trajectories showed that air masses were transported from Mainland China and neighbouring regions. In Mainland China and neighbouring regions, this is dry season. During the dry season in this region there are a lot of fires, as reported by Zhang et al. (2015) and Ho et al. (2014), and this influences the pollution of air masses transported to the present location. This scenario of biomass fire hotspots is commonly noticed in these two seasons. In past years Malaysia and Singapore have experienced intensified haze episodes in this particular season, e.g. 1997, 2005, 2013, and 2015. A study of this area by Kanniah et al. (2014) observed that during the dry season (June to September) aerosols mainly originated from the west and south-west (i.e. Sumatra, Indonesia), while during the wet season (November to March) aerosols were mostly associated with the NE monsoon winds coming from the South China Sea. Also, the variability of BLH and wind speed (WS) were able to influence the concentration of the pollutants at a particular location. Figure 4 shows the day to day variation of BLH and WS with respect to the 24 h average of $PM_{2.5}$ concentration. From the plot, it is revealed that the daily average $PM_{2.5}$ concentration is inversely proportional to the BLH. Therefore, while factors such as traffic volume, industrial emissions, power plants, land use, and population size can alter the concentration of $PM_{2.5}$, meteorological factors, which govern the day to day variation of BLH in Peninsular Malaysia, might play a crucial role too. These meteorological factors can include strong local convection, which is a very common meteorological feature in this region, and also the movement of air via a land–sea breeze due to the sea surrounding Peninsular Malaysia. A study by Lelieveld et al. (2001) reported that strong convection can ventilate the daily BLH. The small expansion of BLH that was observed during NE monsoon was most likely due to the higher magnitude of WS to Peninsular Malaysia during this season, as demonstrated in Fig. 2.

In comparison, our results of $PM_{2.5}$ here on the west coast of Peninsular Malaysia (avg $= 25.13 \, \mu g \, m^{-3}$) are higher compared to the east coast of Peninsular Malaysia at $14.3 \, \mu g \, m^{-3}$ (Mohd Tahir et al., 2013). This $PM_{2.5}$ concentration in this study area was similar to the annual concentration of $PM_{2.5}$ measured in Petaling Jaya, Kuala Lumpur ($26.85 \, \mu g \, m^{-3}$) by Rahman et al. (2011), Petaling Jaya ($33 \, \mu g \, m^{-3}$) and Gombak ($28 \, \mu g \, m^{-3}$) by Keywood et al. (2003) and Singapore ($27.2 \, \mu g \, m^{-3}$) as reported by Balasubramanian et al. (2003). The yearly mean value of $PM_{2.5}$ in the Bandung urban area and suburban location in Lembang of Indonesia are 14.03 and $11.88 \, \mu g \, m^{-3}$, respectively (Santoso et al., 2008), which are much lower concentration compared to the this study. However, Lestari and Mauliadi (2009) reported that the $PM_{2.5}$ concentration of $43.5 \, \mu g \, m^{-3}$ in the Bandung city, Indonesia, was about

1.7 times larger than that of the current location and by Budhavant et al. (2015) showed $19 \, \mu g \, m^{-3}$ in Male, Maldives (urban), which is lower as well compared to this study. A comparative study conducted in Bangkok ($34 \, \mu g \, m^{-3}$), Beijing ($136 \, \mu g \, m^{-3}$), Chennai ($44 \, \mu g \, m^{-3}$), Bandung ($45.5 \, \mu g \, m^{-3}$), Manila ($43.5 \, \mu g \, m^{-3}$), and Hanoi ($78.5 \, \mu g \, m^{-3}$) showed consistently higher $PM_{2.5}$ pollution in the Southeast and South Asian cities as compared to this study (Kim Oanh et al., 2006). From Table 1, it can be seen that the highest concentration of anions species was found for SO_4^{2-} followed by NO_3^-. A study by Zhang et al. (2012) suggested that the photochemical conversion of SO_2 to H_2SO_4 is the main reason for the changes of sulfate concentration in $PM_{2.5}$ and that higher temperatures reduce the nitrate concentration by the partitioning of nitrate into the gas phase. However, lower temperatures and a stable atmosphere favours the formation of NO_3^- aerosol reacting with NH_4^+, i.e. shifting the gas phase nitrate into the particle phase (Mariani and de Mello, 2007). The formation of NH_4NO_3 normally occurs at high humidity with lower temperatures (Morales and Leiva, 2006). The average molar ratios of SO_4^{2-} to NO_3^- were 6.0 with a range of 0.16–38.24, which suggests that the sulfate aerosol is more dominant over the nitrate aerosol and may have been transported from trans-boundary sources. A similar observation was found in a study in the UK by Abdalmogith and Harrison (2006). This ion balance ratio indicates the possible sources of aerosol, and stationary sources dominate over the mobile sources as explained by Arimoto et al. (1996). The average ratio of SO_4^{2-} to NH_4^+ was 1.28, which is much higher than the ratio of NO_3^- to NH_4^+ (0.63), confirming that the sulfate aerosol is more stable in tropical conditions as compared to the nitrate aerosol. A study by Maenhaut et al. (2008) described a similar observation. The formation of ammonium sulfate is favoured in the fine fraction (Khan et al., 2010b). For the cations, the highest concentration was NH_4^+ followed by Na^+. However, the average molar ratio of Cl^- to Na^+ did not reflect the seawater ratio. "Cl loss" may be the cause of the drop in Cl^- to Na^+ ratio. Boreddy et al. (2014) also noticed a chlorine depletion due to atmospheric processing in the western North Pacific. According to Finlayson-Pitts and Pitts (2000), sulfuric and nitric acids have a tendency to react rapidly with NaCl, the major component of sea salt particles, to produce gaseous HCl under 50–100 % relative humidity conditions. For heavy metals, the predominant metal reported was Fe with concentrations in the range 2171–$4567 \, ng \, m^{-3}$. Ca showed the second-highest concentrations with the concentration range of below MDL – $3150 \, ng \, m^{-3}$. A study by Yin and Harrison (2008) suggested that Fe originates from non-traffic sources and that iron and calcium are released into ambient air through the resuspension of surface dust. Among other heavy metals of particular health concern, the average concentrations of As, Pb, Cd, Mn, Ni, V, and Cr were 5.76, 21.84, 0.54, 4.03, 17.24, 5.13, and $107.68 \, ng \, m^{-3}$, respectively. The As concentration was
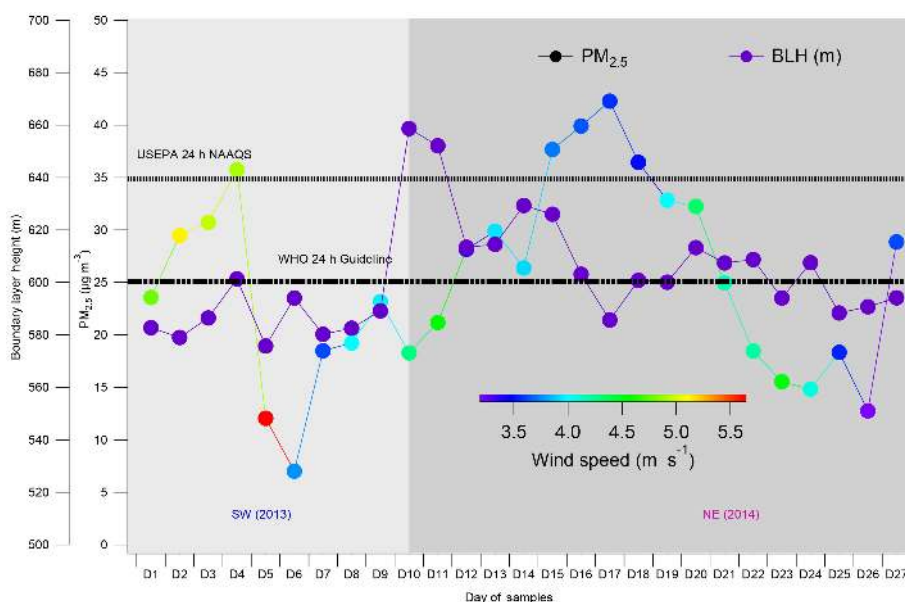
Figure 4. Time series of 24 h averages of PM$_{2.5}$, wind speed (m s^{-1}), and yearly daily mean of the boundary layer height (BLH) over the region of Peninsular Malaysian.

nearly equal to the WHO and US EPA guideline values of 6.6 and 6 ng m^{-3}, respectively. Therefore, As may be of significant health concern. The concentrations of other hazardous metals were well below the WHO and European commission guidelines. The EF reveals that all metals of PM$_{2.5}$ can be assumed to originate from anthropogenic sources with no seasonal differences observed (Fig. 5a).

3.2   Mass closure model

The PM$_{2.5}$ was reconstructed by the use of a PMC model (Harrison et al., 2003). Employing the mass closure model outlined in the previous section, the four major classes of chemical components contributing to PM$_{2.5}$ were (i) MIN, (ii) SIA, (iii) SS, (iv) TE, and UD. As shown in Fig. 5c, the overall reconstructed masses of MIN, SIA, SS, TE, and UD were 8970, 2841, 1727, 626.2, and 11511 ng m^{-3}, respectively. MIN is released from soil or crustal sources and represents the oxide form of the metals (Remoundaki et al., 2013; Sillanpää et al., 2006; Terzi et al., 2010). The MIN component comprises 35 % of the PM$_{2.5}$ concentration. SIA, which accounts for 11 %, is comprised of the most abundant secondary ions (nss-SO$_4^{2-}$, NO$_3^-$ and NH$_4^+$). These are formed in the atmosphere from the precursor gases (SO$_2$, NH$_3$ and NO$_x$) through a gas-to-particle conversion (Sillanpää et al., 2006) and therefore are assumed to be in the form of (NH$_4$)$_2$SO$_4$ and NH$_4$NO$_3$ in the aerosol phase (Joseph et al., 2012). It is important to mention that the behaviour of the formation pattern of the SIA in this Southeast Asia region may differ from other regions due to the nearly constant temperature throughout the year. SS and TE accounted for 7

and 2 % of the PM$_{2.5}$. The UD, undefined fraction, accounted for 45 % of PM$_{2.5}$.

The average value of reconstructed PM$_{2.5}$ by mass closure (MC) is 14.12 ± 4.32 μg m^{-3} with a minimum of 6.70 μg m^{-3} and a maximum of 24.19 μg m^{-3}. On the other hand, the measured PM$_{2.5}$ determined gravimetrically by HVS was 25.13 ± 9.21 μg m^{-3} with a range of 7.01 to 42.28 μg m^{-3}. A correlation plot of PM$_{2.5}$ (MC) and measured PM$_{2.5}$ (HVS) is shown in Fig. 5e. The correlation shows a good fit ($r^2 = 0.98$) with a slope of 0.46 and an intercept of 1.93. The results of the fit parameters suggest that the PM$_{2.5}$ mass (MC) concentration was underestimated compared to PM$_{2.5}$ (HVS). The reported result of the mass closure model is based on the analysed chemical components of filter samples ($\sim$ 55 %). As described in the mass closure, a large portion of PM$_{2.5}$ mass ($\sim$ 45 %) was left unidentified; this unidentified component is believed to be the organics or carbonaceous species. Elemental carbon (EC), organic carbon (OC) and water-soluble organics were not measured due to the lack of instrumentation. Other possible reasons for the un-identified portion are (i) unaccounted for mineral oxides as they are abundant in PM$_{2.5}$, and (ii) water associated with salts.

During the SW monsoon, the UD showed the higher concentrations; this can be explained by the annual biomass haze episodes experienced in this area. Thus, a large proportion of the UD of PM$_{2.5}$ is probably formed from the organic fraction. Such findings are consistent with a study conducted by Abas and Simoneit (1996), which also found that the concentrations of organic compounds observed were greater during the haze episodes than any other periods in a year, and that
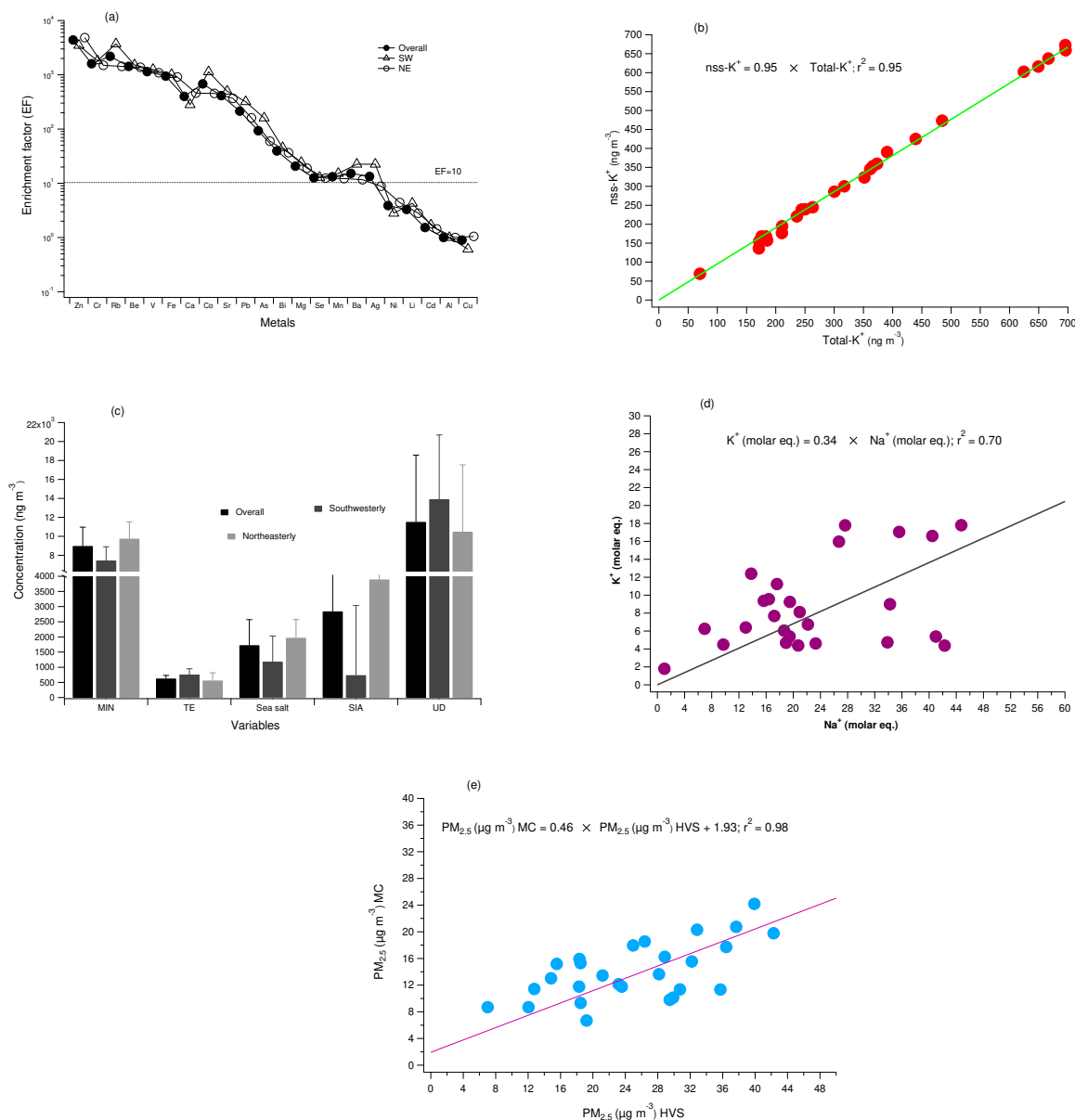
Figure 5. (a) Enrichment factor (EF) of heavy metals in PM$_{2.5}$, **(b)** correlation plot of nss-K$^+$ and total K$^+$, **(c)** reconstructed mass concentration of PM$_{2.5}$ by mass closure model, **(d)** correlation plot of K$^+$ and Na$^+$, and **(e)** correlation plot of estimated PM$_{2.5}$ (MC) and measured PM$_{2.5}$ (HVS).

some of them are suspected to be transported from transboundary sources.

The seasonal variability of the results obtained from the mass closure model is shown in Fig. 5c. The reconstructed masses of MIN, SIA, and SS were higher in the NE than the SW monsoon. These haze events were very likely caused by the slash-and-burn activities practiced by the agriculture industries, and the occurrence of forest fires during this dry season. The regional trans-boundary pollution during the NE and SW monsoon is the underlying reason for the change in

the chemical component concentrations as well as the overall PM$_{2.5}$.

3.3 Identification and apportionment of PM$_{2.5}$ sources

Using US EPA PMF 5.0, the five identified sources of PM$_{2.5}$ were (i) mineral and road dust, (ii) motor vehicle emissions and biomass burning, (iii) nitrate aerosol, (iv) coal burning, and (v) marine and sulfate aerosol. Each of the source profiles is shown in Fig. 6a, which demonstrates the concentration and percentage of the variables to each factor. The reported PMF analysis is based on the chemical components
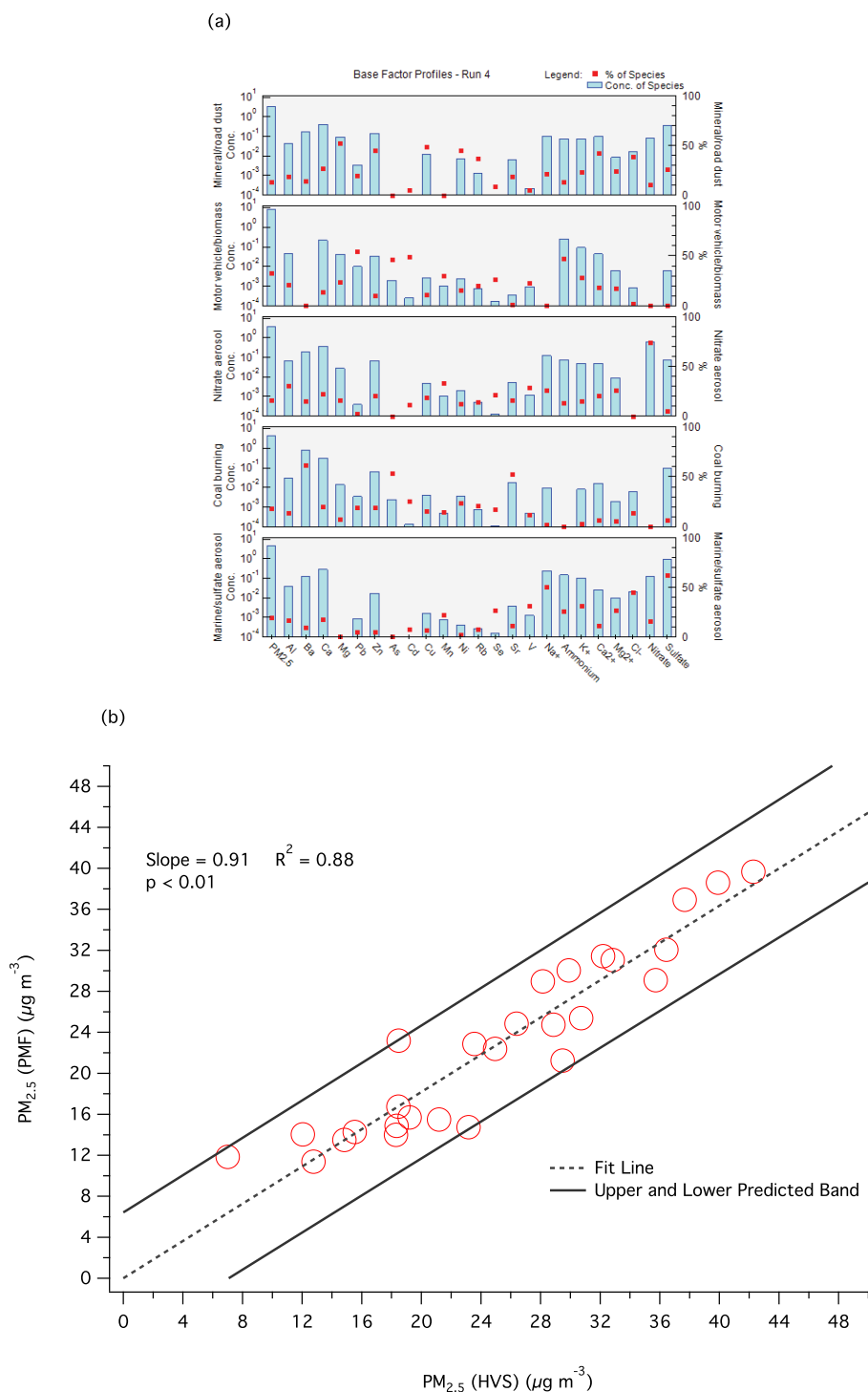
(a)

(b)

Figure 6. (a) The source profiles of $PM_{2.5}$ by positive matrix factorization model and **(b)** comparison of $PM_{2.5}$ (PMF) and $PM_{2.5}$ (HVS).

of filter samples. As described in the mass closure, a large portion of the $PM_{2.5}$ mass fraction (about 45 %) was not apportioned. In the PMF 5.0 procedure, the contributions of five factors were estimated and then the integrated contribution of the five factors was regressed over the measured $PM_{2.5}$

(HVS). The regression fit line was forced through the origin. Thus, our regression of the $PM_{2.5}$ (PMF) and $PM_{2.5}$ (HVS) showed that the $PM_{2.5}$ had been reproduced by PMF 5.0 with an error of less than 10 % and the correlation of $PM_{2.5}$ (PMF) and $PM_{2.5}$ (HVS) showed a strong and significant correla-

tion (slope $= 0.91$, $r^2 = 0.88$, $p < 0.01$) (Fig. 6b). To evaluate the results of the PMF model, the regression between predicted and observed data for each variable is shown during the operation. A linear correlation between the predicted and measured mass represents the goodness-of-fit of linear regression. Our values strongly suggested that the five identified sources could be readily interpreted.

Factor component one: the predominant tracers are Mg, Zn, Cu, Ni, and Ca^{2+}. The mineral or natural fugitive dust component is identified based on the presence of Mg (52 % of the Mg mass), Ca^{2+} (42 % of Ca^{2+} mass), Ca (28 % of Ca mass), and Al (19 % of Al mass), as shown in Table 2. Many other researchers cite these metals as markers for a mineral dust source (Dall'Osto et al., 2013; Moreno et al., 2013; Mustaffa et al., 2014; Viana et al., 2008; Waked et al., 2014). The possible cause of the mineral dust is the rapid development activities of things such as construction, renovation of road surface, etc., around this suburban region. Airborne soil and construction material are the key sources of mineral dust (Dai et al., 2013; Gugamsetty et al., 2012; Huang et al., 2014). Cu, Zn, and Ba are associated with road dust due to the release of these metal markers from cars and from non-exhaust sources (Amato et al., 2011). Several studies identified that Cu is released from brake wear or the brake pads/tailpipes of cars (Wåhlin et al., 2006) while Zn originates from tire wear (Dall'Osto et al., 2013) and additives in cars as lubricant (Ålander et al., 2005). A study by Wang and Hopke (2013) suggested that Ni was emitted from gasoline engine and road dust sources. Ni (48 % of Ni mass) and V (5 % of V mass) are moderately presented in this factor component, which shows the existence of heavy lubricating oil combustion (Amato et al., 2011). The average contribution of mineral or natural fugitive and road dust sources to the $PM_{2.5}$ was 3.17 µg m^{-3} or 13 %.

Factor component two: contains substantial Pb, NH_4^+, and K^+. Motor vehicle emissions and biomass burning sources accounted for 7.47 µg m^{-3} or 31 % of the total $PM_{2.5}$ concentration, which makes these the largest sources contributing to the $PM_{2.5}$ concentration. Pb along with the moderately enriched metals As, Cd, Zn, Ni, and V (Fig. 5a, refer to previous section for detail), represents a motor vehicle emission source (Wu et al., 2007). The brake wear dust of motor vehicles contains Pb (Garg et al., 2000). A study by Begum et al. (2010) conducted in Dhaka and by Santoso et al. (2013) at roadsides in Jakarta defined Pb in $PM_{2.5}$ releasing from the pre-existing road dust by PMF. Choi et al. (2013) also introduced Pb in $PM_{2.5}$ as a tracer for the motor vehicle source. Zn is released from the wear and tear of tyres (Srimuruganandam and Shiva Nagendra, 2012). Further, Zn in $PM_{2.5}$ appeared to have a motor vehicle source as resolved by PMF, due to its use as fuel detergent and anti-wear additive (Brown et al., 2007). Ni and V were widely reported in the literature as markers for the combustion of engine oil or residual oil combustion (Gugamsetty et al., 2012; Han et al., 2006; Huang et al., 2014; Yu et al., 2013). Pb is no longer used

as an additive in gasoline fuel. Thus, the Pb does not reflect the emissions from engine combustion but does reflect those from a non-exhaust traffic source. A study conducted by Rahman et al. (2011) in Kuala Lumpur investigating Pb in $PM_{2.5}$ found that it originated from the soil dust source, indicating the influence of road dust. Also, coal combustion is a predominant source of Pb (Tao et al., 2014). The K^+ ion has been widely cited in the literature as an excellent tracer representing a wood or biomass burning source (Dall'Osto et al., 2013; Kim and Hopke, 2007; Mustaffa et al., 2014; Wahid et al., 2013). The biomass burning source is generally comprised of either wood burning as residential fuel, agriculture residue/waste, and/or wild forest fires. In Kuala Lumpur, the biomass burning source was described due to the presence of K from $PM_{2.5}$ measured by particle-induced X-ray emission (Rahman et al., 2011). During the episode of biomass burning in Chengu, China, K^+ and other related tracers in $PM_{2.5}$ were increased by a factor of 2–7. In this suburban region, the smoke emissions released due to the burning of wheat straw, rape straw, and other biomass fuel for domestic cooking or heating purposes (Tao et al., 2013). K^+ is also mainly emitted from biomass burning in the suburb of Shenzhen, China (Dai et al., 2013), Beijing, China (Yu et al., 2013; Zhang et al., 2013), and Colombo, Sri Lanka (Seneviratne et al., 2011). In Seoul, Korea, biomass burning is characterized by the presence of K and other related markers in $PM_{2.5}$. The character of burning in this East Asian city is typically post-harvest field burning, biofuel burning for heating and cooking as well as forest fire from the outside of the city (Heo et al., 2009). Thus, the local and regional transport of smoke from the burning sources contribute to this factor. Hong Kong experiences the influence of biomass burning in $PM_{2.5}$ due to its trans-boundary origin (Huang et al., 2014). During the sampling period in the SW monsoon, the MODIS detected a very high number of fire counts over the Sumatra Island. In this monsoon season, the wind will consistently travel from the south-west direction, bringing air masses from these burning areas to Peninsular Malaysia. During the NE monsoon, on the other hand, the wind will travel from the north-east direction, bringing air masses from the China mainland, Indochina, and the Philippines to Peninsular Malaysia. In this period of time, a high density of fire locations were found on the Indo-China and China mainland. Zhang et al. (2015) demonstrate that during the dry season there is important biomass burning activity in the Pearl River Delta (China), which can result in trans-border transport and a regional scale character of biomass burning. Therefore, under the north-east monsoonal regime it is possible that outflow from that area can maybe influence the specific area. A study by Streets et al. (2003) estimated that China contributes 25 % to the total biomass burning in Asia and showed a good agreement between national estimate of biomass burning and adjusted fire count. Yang et al. (2013) applied spatial–temporal features of fire counts and observed that the study area of Heilongjiang Province, China was seriously affected by forest fires during

2000–2011. Reid et al. (2013) reported a high intensity of fire counts in Vietnam–China region in April and in Indonesia during September. Khan et al. (2015a) also reported a high density of fire locations in Thailand, Vietnam, and Laos during February and Sahani et al. (2014) reported many in the same regions during June-September. The biomass burning is the dominant source of trace gas and particulate matter and the fire emissions are mainly concentrated in Indonesia, Thailand, Myanmar, and Cambodia (Chang and Song, 2010). Further, a comparison of nss-K^+ with the respective total K^+ is shown in Fig. 5b. The correlation of nss-K^+ as a function of total K^+ showed a strong correlation coefficient ($r^2 = 0.95$), which suggests that K^+ can be used as a biomass tracer. K^+ may also be emitted from local fire sources. Additionally, the molar equivalent of K^+ and Na^+, as shown in Fig. 5c, demonstrated significant correlation ($r^2 = 0.70$) with a slope value of 0.34, which is much higher compared to 0.0225–0.230 and 0.0218, reported by Wilson (1975) and Hara et al. (2012), respectively. The higher molar ratio of K^+ and Na^+ indicates that at the current location, Na^+ depletion was high and the K^+ might also release from other dominant sources. Additional significant sources of K^+, which may attribute to the mass, are soil dust, sea salt, vegetation, and meat cooking (Zhang et al., 2010).

Factor component three: this factor is mainly dominated by the concentration of the nitrate ion (75 % of NO_3^- mass) suggesting that this source is strongly related to the formation of nitrate aerosol. NO_3^- is mainly formed from the conversion of NOx, which is emitted from the exhaust of motor vehicles (Dai et al., 2013). Huang et al. (2014) also identified a nitrate source in PM$_{2.5}$ by the use of PMF in suburban areas of Hong Kong. In Beijing, a nitrate source appeared in PM$_{2.5}$ when source apportionment was performed by PMF (Song et al., 2006). This source is also contributed to by the small amount of Al, Mn and Ca^{2+}. Overall, it accounted for 4.11 µg m^{-3} or about 17 % of the PM$_{2.5}$ concentration.

Factor component four: this fourth source has an abundance of As, Ba, and Sr (Se moderately contributed) and thus is classified as coal burning source. As constitutes the most to this fourth component at 53 % (of As mass), which gives an indication that this source is related to coal combustion. In Malaysia, several power plants are operating on the west coast of Peninsular Malaysia, e.g. Port Dickson, Kapar, and Manjung. The power plants located at Port Dickson and Kapar are about 50 km away from the sampling station. These plants use coal as the raw material to generate electric power. Other researchers have also used As a tracer for the coal burning source (Moreno et al., 2013) and As and Se by Meij and te Winkel (2007) and Querol et al. (1995). As and Se are categorized as of great concern and Ba and Sr are of moderate environmental concern in the utilization of coal, as reported by Vejahati et al. (2010). However, Ba is an indicator of brake wear and tear from motor vehicles (Gietl et al., 2010). Overall, the coal burning source accounts for 4.60 µg m^{-3} or about 19 % of PM$_{2.5}$.

Factor component five: this component features Na^+ (50 % of Na^+ mass), Cl^- (46 % of Cl^- mass), and sulfate (64 % of SO_4^{2-} mass) suggesting the presence of marine as well as sulfate aerosol. Begum et al. (2010) identified sea salt in PM$_{2.5}$ by PMF in Dhaka, based on the appearance of Na and Cl. Choi et al. (2013) defined a sea salt source in Seoul, Korea, due to the high contribution of Na^+ and Cl^- in PM$_{2.5}$. Several other studies in East, Southeast and South Asia assigned a sea salt source in PM$_{2.5}$ considering Na^+ and Cl^- from the model output of PMF (Lee et al., 1999; Santoso et al., 2008, 2013; Seneviratne et al., 2011). For sulfate, it shows that nss-SO_4^{2-} contributed 93 % to the total sulfate concentration while ss-SO_4^{2-} accounted for only 6 %. Therefore, the sulfate aerosol in PM$_{2.5}$ is released as a product from the photochemical conversion of SO_2, which mainly originates from anthropogenic, large point sources as observed by Heo et al. (2009) in Seoul, South Korea. A secondary sulfate source in PM$_{2.5}$ was also identified by Huang et al. (2014) in a suburban area of Hong Kong and by Song et al. (2006) in Beijing. The marine and sulfate aerosol, as the final identified source, accounts for 4.99 µg m^{-3} or about 20 % of the total PM$_{2.5}$ concentration. A study by Kim and Hopke (2007) defined a sea salt source by the high concentration of Na^+ and Cl^-, while sulfate sources are based on the high concentration of sulfate. The secondary aerosol fraction is an important source worldwide, which is also the case here. It generally constitutes a predominant portion of PM$_{2.5}$, which splits into two modes, i.e. the nitrate-rich and sulfate-rich factors. Studies by Chen et al. (2007) and McGinnis et al. (2014) also identified the major contribution of the secondary aerosol fraction to PM$_{2.5}$.

3.4 Health risk implications

Table 3 shows the non-carcinogenic (represented as HQ) and carcinogenic risks posed by several selected metals (Pb, As, Cd, Cu, Mn, Zn, and Ni) in PM$_{2.5}$ mass concentration through inhalation exposure associated with sources. The HQ values for As and Ni in PM$_{2.5}$ mass concentration are 15.9×10^{-2} and 14.3×10^{-2}, respectively, suggesting the non-carcinogenic health risks posed by these metals might be higher compared to other metals. The HQ for four selected metals (Pb, As, Cd, and Ni) in PM$_{2.5}$ mass was the highest in the PM$_{2.5}$ mass originating from a coal burning source and the least in PM$_{2.5}$ originating from a mineral/road dust source. The cut-off point for significant health risks or the safe level to the exposed population is HQ > 1. Our results showed that the sum of HQ for each metal are lower than the safe level (= 1) in PM$_{2.5}$ mass concentration originating from each source. The sum of HQ for PM$_{2.5}$ is 35.7×10^{-2}, which is lower than the HQs of PM$_{2.5}$ reported by Hu et al. (2012) in Nanjing, China (2.96); Cao et al. (2014) in Shanxi Province, China ($1.06 \times 10^{+1}$); and Taner et al. (2013) in a non-smoking restaurant in Turkey (4.09). A study by Hu et al. (2012) reported HQ values for As and Ni in PM$_{2.5}$ as 4.14×10^{-1}

Table 3. Hazard quotient (HQ) and lifetime carcinogenic risk (LCR) for selected heavy metals in $PM_{2.5}$ associated with sources.

Inhalation	Mineral/road dust		Motor vehicle/biomass		Coal burning		$PM_{2.5}$	
	HQ	LCR	HQ	LCR	HQ	LCR	HQ	LCR
Pb	–	4.0×10^{-8}	–	1.0×10^{-7}	–	4.1×10^{-8}	–	2.5×10^{-7}
As	1.8×10^{-3}	1.1×10^{-7}	4.9×10^{-2}	1.1×10^{-6}	6.6×10^{-2}	1.5×10^{-6}	15.9×10^{-2}	3.5×10^{-6}
Cd	4.6×10^{-4}	8.2×10^{-9}	9.1×10^{-3}	5.6×10^{-8}	5.5×10^{-3}	3.4×10^{-8}	2.2×10^{-2}	1.4×10^{-7}
Cu	–	–	–		–		–	
Mn	–	–	7.0×10^{-3}		5.1×10^{-3}		3.3×10^{-2}	
Zn	–	–	–		–		–	
Ni	2.0×10^{-2}	2.5×10^{-7}	2.3×10^{-2}	9.5×10^{-8}	2.6×10^{-2}	1.1×10^{-7}	14.3×10^{-2}	5.9×10^{-7}
THR (HI and LCR)	2.3×10^{-2}	1.6×10^{-7}	8.8×10^{-2}	1.2×10^{-6}	10.2×10^{-2}	1.5×10^{-6}	35.7×10^{-2}	3.9×10^{-6}

Pb: Pb (acetate); As: As (Inorganic); Cd: Cd (Diet); Mn: Mn (Diet); Zn: Zn (Metallic); Ni: Ni (Refinery Dust); "–": no data; THR: total health risk; HI: hazard index; LCR: lifetime cancer risk.

and 1.73×10^{-1}, respectively, in Nanjing, China. However, the HQs of $PM_{2.5}$ estimated after inhalation at two sites in Nanjing City, China (0.88, Xianlin, and 0.79, Gulou), were close to the safe level ($= 1$) according to a study by Y. Li et al. (2015). At two urban locations in Yangtze River Delta, China, the HQ for Cr in $PM_{2.5}$ was within the acceptable limit but higher for Mn (Niu et al., 2015). Although the HQ calculated for As was the highest, it was below 1; thus, the non-carcinogenic health risk was estimated to be at a safe level. In addition, the hazard index (total-hazard quotient) of $PM_{2.5}$ calculated for the four heavy metals (As, Cd, Mn, Ni) from the different sources (Table 3) showed an insignificant health risk.

The carcinogenic risks from the carcinogenic heavy metals Pb, As, Cd, and Ni in $PM_{2.5}$ are shown in Table 3. Similar to the non-carcinogenic risks, the lifetime carcinogenic risk level is estimated for $PM_{2.5}$ mass concentration and may be contributed to by several heavy metals from different sources: mineral/road dust, motor vehicle emissions/biomass burning and coal combustion. The total LCR from heavy metals in the $PM_{2.5}$ mass concentration was calculated at 3.9×10^{-6}, which is a significant cancer risk. The main carcinogenic heavy metal of concern to the health of people at the current location is As; the other heavy metals (Ni, Pb, and Cd) did not pose a significant cancer risk. Thus, the LCR from the $PM_{2.5}$ mass concentration originating from motor vehicle/biomass and coal burning sources showed a value of 1×10^{-6}, slightly above the acceptable cancer risk level as recommended by USEPA, while the total LCR from $PM_{2.5}$ mass concentration from all sources was estimated to be 4×10^{-6}, which is also slightly above the acceptable cancer risk. The carcinogenic risk posed by As (3.66×10^{-3}) in $PM_{2.5}$ in Shanxi Province, China (Cao et al., 2014), was higher than the guideline value set by USEPA. A study by Niu et al. (2015) of $PM_{2.5}$-bound metals showed a high cancer risk in Yangtze River Delta, China (2.47×10^{-4}). A study by Pandey et al. (2013) conducted in the vicinity of human activities observed that the concentrations of Cd, Cr, Ni, and

Pb in $PM_{2.5}$ showed higher excess cancer risk (ECR) due to those particle-bound metals compared to guideline level set by USEPA. Satsangi et al. (2014) also reported a higher cancer risk from Cr, Ni and Cd in $PM_{2.5}$ compared to the USEPA guideline. The integrated carcinogenic risk of six metals (Cr, As, Co, Pb, Ni, and Cd) in $PM_{2.5}$ in Tianjin, China were in the range 3.4×10^{-3}–4.1×10^{-3}, which is reportedly beyond the tolerance level (Zhang et al., 2014). The total ECRs based on the average values of As, Cd, Cr, Ni, and Pb in $PM_{2.5}$ is 4.34×10^{-5} in Delhi, India, implying that four or five people might get cancer out of 100 000 people after exposure to toxic metals in $PM_{2.5}$ (Khanna et al., 2015). Our findings showed that the lifetime cancer risk posed by the exposure of heavy metals in $PM_{2.5}$ mass concentration is 3–4 per 1 000 000 people at this location. This significant cancer risk warrants further investigation. Our findings showed that an insignificant non-carcinogenic risk and significant cancer risk is posed to the population from exposure to $PM_{2.5}$ at this location. Detailed exposure assessment of the $PM_{2.5}$ at the specific sources and the health risks posed by individual hazardous elements of concern may help to improve understanding about the exposure pathways as well as the detailed risk factors involved in both carcinogenic and non-carcinogenic risk.

4 Conclusions

$PM_{2.5}$ samples were collected using a high-volume sampler in a semi-urban site on Peninsular Malaysia. The results obtained for $PM_{2.5}$ showed that 48 % of the samples exceeded the WHO 24 h guideline and 19 % exceeded the US EPA 24 h NAAQS for $PM_{2.5}$. The average value of $PM_{2.5}$ is higher than a previous study carried out on the east coast of Peninsular Malaysia. $PM_{2.5}$ concentration during the NE monsoon was slightly higher than the SW monsoon with air masses from different origins. For the SW monsoon the air masses originated from Sumatera, Indonesia, and for the NE monsoon from southern China. Major carcinogenic metals, namely As,

Pb, Cr, Ni, and Cd, have contributed to $PM_{2.5}$ by a significant portion. Of all carcinogenic metals, As was close to the values set by the WHO and EU guidelines.

Results of the EF analysis suggested that a large number of the heavy metals in $PM_{2.5}$ emitted from anthropogenic sources. No seasonal differences were found in the EF of the heavy metals. The mass closure model results showed higher MIN, SIA, and SS in the NE than the SW monsoon. Further analysis revealed that sulfate is relatively more stable in tropical climates compared to nitrate aerosol, indicating the dominance of static sources over mobile sources. However, the average molar ratio of Cl^- to Na^+ does not reflect the seawater ratio. "Cl loss" may be the cause of the drop in Cl^- to Na^+ ratio. The five sources of $PM_{2.5}$ obtained by the PMF 5.0 model were dominated by motor vehicle emissions/biomass burning ($7.47 \mu g\, m^{-3}$, 31 %). The other four sources were mineral/road dust; nitrate aerosol; coal burning; and marine-sulfate aerosol with an overall contribution of $3.17 \mu g\, m^{-3}$ (13 %), $4.11 \mu g\, m^{-3}$ (17 %), $4.60 \mu g\, m^{-3}$ (19 %), and $4.99 \mu g\, m^{-3}$ (20 %), respectively.

Using the PMF-identified sources as the basis, the hazard quotient (HQ) for four selected metals (Pb, As, Cd and Ni) in $PM_{2.5}$ mass was the highest in $PM_{2.5}$ originating from a coal burning source and the least in that originating from a mineral/road dust source. The non-carcinogenic cancer risk posed by the exposure of $PM_{2.5}$ was at a considerably safer level compared to the South and East Asian region. The lifetime cancer risk (LCR) followed the order of As > Ni > Pb > Cd for mineral/road dust, coal burning sources and $PM_{2.5}$ mass concentration, and As > Pb > Ni > Cd for motor vehicle/biomass burning. Among the trace metals studied, As predominantly showed the largest LCR in $PM_{2.5}$ mass concentration as well as its associated sources, implying the largest risk after exposure of $PM_{2.5}$ to people at the current location. The associated LCR posed by the exposure of the hazardous metals in $PM_{2.5}$ mass concentration was 3–4 per 1 000 000 people at this location. This significant LCR warrants further investigation. Detailed exposure assessment of the $PM_{2.5}$ at the specific sources and the health risks posed by individual hazardous elements may help to improve understanding about the exposure pathways as well as the detailed risk factors involved in both carcinogenic and non-carcinogenic risk. Therefore, the motor vehicle emissions and regional trans-boundary pollution were the major underlying reasons for the change in the chemical component of $PM_{2.5}$ in tropical Peninsular Malaysia, which potentially leads to different health threats.

The Supplement related to this article is available online at doi:10.5194/acp-16-597-2016-supplement.

References

Abas, M. R. and Simoneit, B. R. T.: Composition of extractable organic matter of air particles from malaysia: Initial study, Atmos. Environ., 30, 2779–2793, doi:10.1016/1352-2310(95)00336-3, 1996.

Abdalmogith, S. S. and Harrison, R. M.: An analysis of spatial and temporal properties of daily sulfate, nitrate and chloride concentrations at UK urban and rural sites, J. Environ. Monit., 8, 691–699, doi:10.1039/B601562J, 2006.

Ålander, T., Antikainen, E., Raunemaa, T., Elonen, E., Rautiola, A., and Torkkell, K.: Particle Emissions from a Small Two-Stroke Engine: Effects of Fuel, Lubricating Oil, and Exhaust Aftertreatment on Particle Characteristics, Aerosol Sci. Technol., 39, 151–161, doi:10.1080/027868290910224, 2005.

Amato, F., Viana, M., Richard, A., Furger, M., Prévôt, A. S. H., Nava, S., Lucarelli, F., Bukowiecki, N., Alastuey, A., Reche, C., Moreno, T., Pandolfi, M., Pey, J., and Querol, X.: Size and time-resolved roadside enrichment of atmospheric particulate pollutants, Atmos. Chem. Phys., 11, 2917–2931, doi:10.5194/acp-11-2917-2011, 2011.

Anenberg, S., West, J. J., Yu, H., Chin, M., Schulz, M., Bergmann, D., Bey, I., Bian, H., Diehl, T., Fiore, A., Hess, P., Marmer, E., Montanaro, V., Park, R., Shindell, D., Takemura, T., and Dentener, F.: Impacts of intercontinental transport of anthropogenic fine particulate matter on human mortality, Air Qual. Atmos. Health, 7, 369–379, doi:10.1007/s11869-014-0248-9, 2014.

Arimoto, R., Duce, R. A., Savoie, D. L., Prospero, J. M., Talbot, R., Cullen, J. D., Tomza, U., Lewis, N. F., and Ray, B. J.: Relationships among aerosol constituents from Asia and the North Pacific during PEM-West A, J. Geophys. Res., 101, 2011–2023, doi:10.1029/95JD01071, 1996.

Balasubramanian, R., Qian, W. B., Decesari, S., Facchini, M. C., and Fuzzi, S.: Comprehensive characterization of $PM_{2.5}$ aerosols in Singapore, J. Geophys. Res., 108, 4523, doi:10.1029/2002JD002517, 2003.

Baumann, K., Jayanty, R. K. M., and Flanagan, J. B.: Fine Particulate Matter Source Apportionment for the Chemical Speciation Trends Network Site at Birmingham, Alabama, Using Positive Matrix Factorization, J. Air Waste Manage., 58, 27–44, doi:10.3155/1047-3289.58.1.27, 2008.

Begum, B. A., Biswas, S. K., Markwitz, A., and Hopke, P. K.: Identification of sources of fine and coarse particulate matter in Dhaka, Bangladesh, Aerosol Air Qual. Res., 10, 345–353, doi:10.4209/aaqr.2009.12.0082, 2010.

Bell, M. L., Ebisu, K., Leaderer, B. P., Gent, J. F., Lee, H. J., Koutrakis, P., Wang, Y., Dominici, F., and Peng, R. D.: Associations of $PM_{2.5}$ Constituents and Sources with Hospital Admissions: Analysis of Four Counties in Connecticut and Mas-

sachusetts (USA) for Persons ≥ 65 Years of Age, Environ. Health Persp., 122, 138–144, doi:10.1289/ehp.1306656, 2014.

Betha, R., Behera, S. N., and Balasubramanian, R.: 2013 Southeast Asian Smoke Haze: Fractionation of Particulate-Bound Elements and Associated Health Risk, Environ. Sci. Technol., 48, 4327–4335, doi:10.1021/es405533d, 2014.

Birmili, W., Allen, A. G., Bary, F., and Harrison, R. M.: Trace Metal Concentrations and Water Solubility in Size-Fractionated Atmospheric Particles and Influence of Road Traffic, Environ. Sci. Technol., 40, 1144–1153, doi:10.1021/es0486925, 2006.

Boldo, E., Linares, C., Lumbreras, J., Borge, R., Narros, A., García-Pérez, J., Fernández-Navarro, P., Pérez-Gómez, B., Aragonés, N., Ramis, R., Pollán, M., Moreno, T., Karanasiou, A., and López-Abente, G.: Health impact assessment of a reduction in ambient $PM_{2.5}$ levels in Spain, Environ. Int., 37, 342–348, doi:10.1016/j.envint.2010.10.004, 2011.

Boreddy, S. K. R., Kawamura, K., and Jung, J.: Hygroscopic properties of particles nebulized from water extracts of aerosols collected at Chichijima Island in the western North Pacific: An outflow region of Asian dust, J. Geophys. Res.-Atmos., 119, 167–178, doi:10.1002/2013JD020626, 2014.

Brown, S. G., Frankel, A., Raffuse, S. M., Roberts, P. T., Hafner, H. R., and Anderson, D. J.: Source Apportionment of Fine Particulate Matter in Phoenix, AZ, Using Positive Matrix Factorization, J. Air Waste Manage., 57, 741–752, doi:10.3155/1047-3289.57.6.741, 2007.

Brown, S. G., Lee, T., Norris, G. A., Roberts, P. T., Collett Jr., J. L., Paatero, P., and Worsnop, D. R.: Receptor modeling of near-roadway aerosol mass spectrometer data in Las Vegas, Nevada, with EPA PMF, Atmos. Chem. Phys., 12, 309–325, doi:10.5194/acp-12-309-2012, 2012.

Budhavant, K., Andersson, A., Bosch, C., Kruså, M., Murthaza, A., Zahid, and Gustafsson, Ö.: Apportioned contributions of $PM_{2.5}$ fine aerosol particles over the Maldives (northern Indian Ocean) from local sources vs long-range transport, Sci. Total. Environ., 536, 72–78, doi:10.1016/j.scitotenv.2015.07.059, 2015.

Cao, S., Duan, X., Zhao, X., Ma, J., Dong, T., Huang, N., Sun, C., He, B., and Wei, F.: Health risks from the exposure of children to As, Se, Pb and other heavy metals near the largest coking plant in China, Sci. Total. Environ., 472, 1001–1009, doi:10.1016/j.scitotenv.2013.11.124, 2014.

Chang, D. and Song, Y.: Estimates of biomass burning emissions in tropical Asia based on satellite-derived data, Atmos. Chem. Phys., 10, 2335–2351, doi:10.5194/acp-10-2335-2010, 2010.

Chen, L. W. A., Watson, J. G., Chow, J. C., and Magliano, K. L.: Quantifying $PM_{2.5}$ Source Contributions for the San Joaquin Valley with Multivariate Receptor Models, Environ. Sci. Technol., 41, 2818–2826, doi:10.1021/es0525105, 2007.

Chester, R., Nimmo, M., Fones, G. R., Keyse, S., and Zhang, Z.: Trace metal chemistry of particulate aerosols from the UK mainland coastal rim of the NE Irish sea, Atmos. Environ., 34, 949–958, doi:10.1016/S1352-2310(99)00234-4, 2000.

Cheung, K., Shafer, M. M., Schauer, J. J., and Sioutas, C.: Historical trends in the mass and chemical species concentrations of coarse particulate matter in the Los Angeles Basin and relation to sources and air quality regulations, J. Air Waste Manage., 62, 541–556, doi:10.1080/10962247.2012.661382, 2012.

Choi, J.-K., Heo, J.-B., Ban, S.-J., Yi, S.-M., and Zoh, K.-D.: Source apportionment of $PM_{2.5}$ at the coastal area in Korea, Sci. Total.

Environ., 447, 370–380, doi:10.1016/j.scitotenv.2012.12.047, 2013.

Chueinta, W., Hopke, P. K., and Paatero, P.: Investigation of sources of atmospheric aerosol at urban and suburban residential areas in Thailand by positive matrix factorization, Atmos. Environ., 34, 3319–3329, doi:10.1016/S1352-2310(99)00433-1, 2000.

Cusack, M., Talbot, N., Ondráček, J., Minguillón, M. C., Martins, V., Klouda, K., Schwarz, J., and Ždímal, V.: Variability of aerosols and chemical composition of PM_{10}, $PM_{2.5}$ and PM_1 on a platform of the Prague underground metro, Atmos. Environ., 118, 176–183, doi:10.1016/j.atmosenv.2015.08.013, 2015.

Dai, W., Gao, J., Cao, G., and Ouyang, F.: Chemical composition and source identification of $PM_{2.5}$ in the suburb of Shenzhen, China, Atmos. Res., 122, 391–400, doi:10.1016/j.atmosres.2012.12.004, 2013.

Dall'Osto, M., Querol, X., Amato, F., Karanasiou, A., Lucarelli, F., Nava, S., Calzolai, G., and Chiari, M.: Hourly elemental concentrations in $PM_{2.5}$ aerosols sampled simultaneously at urban background and road site during SAPUSS – diurnal variations and PMF receptor modelling, Atmos. Chem. Phys., 13, 4375–4392, doi:10.5194/acp-13-4375-2013, 2013.

Dee, D. P., Uppala, S. M., Simmons, A. J., Berrisford, P., Poli, P., Kobayashi, S., Andrae, U., Balmaseda, M. A., Balsamo, G., Bauer, P., Bechtold, P., Beljaars, A. C. M., van de Berg, L., Bidlot, J., Bormann, N., Delsol, C., Dragani, R., Fuentes, M., Geer, A. J., Haimberger, L., Healy, S. B., Hersbach, H., Hólm, E. V., Isaksen, L., Kållberg, P., Köhler, M., Matricardi, M., McNally, A. P., Monge-Sanz, B. M., Morcrette, J. J., Park, B. K., Peubey, C., de Rosnay, P., Tavolato, C., Thépaut, J. N., and Vitart, F.: The ERA-Interim reanalysis: configuration and performance of the data assimilation system, Q. J. Roy. Meteor. Soc., 137, 553–597, doi:10.1002/qj.828, 2011.

Finlayson-Pitts, B. J. and Pitts Jr., J. N.: Chemistry of the Upper and Lower Atmosphere: Theory, Experiments, and Applications, Wiley, New York, USA, 2000.

Garg, B. D., Cadle, S. H., Mulawa, P. A., Groblicki, P. J., Laroo, C., and Parr, G. A.: Brake Wear Particulate Matter Emissions, Environ. Sci. Technol., 34, 4463–4469, doi:10.1021/es001108h, 2000.

Gibson, M. D., Haelssig, J., Pierce, J. R., Parrington, M., Franklin, J. E., Hopper, J. T., Li, Z., and Ward, T. J.: A comparison of four receptor models used to quantify the boreal wildfire smoke contribution to surface $PM_{2.5}$ in Halifax, Nova Scotia during the BORTAS-B experiment, Atmos. Chem. Phys., 15, 815–827, doi:10.5194/acp-15-815-2015, 2015.

Gietl, J. K., Lawrence, R., Thorpe, A. J., and Harrison, R. M.: Identification of brake wear particles and derivation of a quantitative tracer for brake dust at a major road, Atmos. Environ., 44, 141–146, doi:10.1016/j.atmosenv.2009.10.016, 2010.

Gugamsetty, B., Wei, H., Liu, C.-N., Awasthi, A., Hsu, S.-C., Tsai, C.-J., Roam, G.-D., Wu, Y.-C., and Chen, C.-F.: Source characterization and apportionment of PM_{10}, $PM_{2.5}$ and $PM_{0.1}$ by using positive matrix factorization, Aerosol Air Qual. Res., 12, 476–491, doi:10.4209/aaqr.2012.04.0084, 2012.

Han, J. S., Moon, K. J., Lee, S. J., Kim, Y. J., Ryu, S. Y., Cliff, S. S., and Yi, S. M.: Size-resolved source apportionment of ambient particles by positive matrix factorization at Gosan background site in East Asia, Atmos. Chem. Phys., 6, 211–223, doi:10.5194/acp-6-211-2006, 2006.

Hara, K., Osada, K., Yabuki, M., and Yamanouchi, T.: Seasonal variation of fractionated sea-salt particles on the Antarctic coast, Geophys. Res. Lett., 39, L18801, doi:10.1029/2012GL052761, 2012.

Harrison, R. M., Jones, A. M., and Lawrence, R. G.: A pragmatic mass closure model for airborne particulate matter at urban background and roadside sites, Atmos. Environ., 37, 4927–4933, doi:10.1016/j.atmosenv.2003.08.025, 2003.

Harrison, R. M., Beddows, D. C. S., and Dall'Osto, M.: PMF Analysis of Wide-Range Particle Size Spectra Collected on a Major Highway, Environ. Sci. Technol., 45, 5522–5528, doi:10.1021/es2006622, 2011.

Hedberg, E., Gidhagen, L., and Johansson, C.: Source contributions to PM_{10} and arsenic concentrations in Central Chile using positive matrix factorization, Atmos. Environ., 39, 549–561, doi:10.1016/j.atmosenv.2004.11.001, 2005.

Henry, R. C.: Current factor analysis receptor models are ill-posed, Atmos. Environ., 21, 1815–1820, doi:10.1016/0004-6981(87)90122-3, 1987.

Heo, J.-B., Hopke, P. K., and Yi, S.-M.: Source apportionment of $PM_{2.5}$ in Seoul, Korea, Atmos. Chem. Phys., 9, 4957–4971, doi:10.5194/acp-9-4957-2009, 2009.

Ho, K. F., Engling, G., Ho, S. S. H., Huang, R., Lai, S., Cao, J., and Lee, S. C.: Seasonal variations of anhydrosugars in $PM_{2.5}$ in the Pearl River Delta Region, China, Tellus B 2014, 66, 22577, doi:10.3402/tellusb.v66.22577, 2014.

Hu, X., Zhang, Y., Ding, Z., Wang, T., Lian, H., Sun, Y., and Wu, J.: Bioaccessibility and health risk of arsenic and heavy metals (Cd, Co, Cr, Cu, Ni, Pb, Zn and Mn) in TSP and $PM_{2.5}$ in Nanjing, China, Atmos. Environ., 57, 146–152, doi:10.1016/j.atmosenv.2012.04.056, 2012.

Huang, X. H., Bian, Q., Ng, W. M., Louie, P. K., and Yu, J. Z.: Characterization of $PM_{2.5}$ major components and source investigation in suburban Hong Kong: A one year monitoring study, Aerosol Air Qual. Res., 14, 237–250, doi:10.4209/aaqr.2013.01.0020, 2014.

Joseph, A. E., Unnikrishnan, S., and Kumar, R.: Chemical characterization and mass closure of fine aerosol for different land use patterns in Mumbai city, Aerosol Air Qual. Res., 12, 61–72, doi:10.4209/aaqr.2011.04.0049, 2012.

Kanniah, K. D., Lim, H. Q., Kaskaoutis, D. G., and Cracknell, A. P.: Investigating aerosol properties in Peninsular Malaysia via the synergy of satellite remote sensing and ground-based measurements, Atmos. Res., 138, 223–239, doi:10.1016/j.atmosres.2013.11.018, 2014.

Keywood, M. D., Ayers, G. P., Gras, J. L., Boers, C. P., and Leong: Haze in the Klang Valley of Malaysia, Atmos. Chem. Phys., 3, 591–605, doi:10.5194/acp-3-591-2003, 2003.

Khan, M. F., Shirasuna, Y., Hirano, K., and Masunaga, S.: Urban and suburban aerosol in Yokohama, Japan: a comprehensive chemical characterization, Environ. Monit. Assess., 171, 441–456, doi:10.1007/s10661-009-1290-1, 2010a.

Khan, M. F., Shirasuna, Y., Hirano, K., and Masunaga, S.: Characterization of $PM_{2.5}$, $PM_{2.5–10}$ and $PM_{>10}$ in ambient air, Yokohama, Japan, Atmos. Res., 96, 159–172, doi:10.1016/j.atmosres.2009.12.009, 2010b.

Khan, M. F., Hirano, K., and Masunaga, S.: Assessment of the sources of suspended particulate matter aerosol using US

EPA PMF 3.0, Environ. Monit. Assess., 184, 1063–1083, doi:10.1007/s10661-011-2021-y, 2012.

Khan, M. F., Latif, M. T., Amil, N., Juneng, L., Mohamad, N., Nadzir, M. S. M., and Hoque, H. M. S.: Characterization and source apportionment of particle number concentration at a semi-urban tropical environment, Environ. Sci. Pollut. Res., 22, 13111–13126, doi:10.1007/s11356-015-4541-4, 2015a.

Khan, M. F., Latif, M. T., Lim, C. H., Amil, N., Jaafar, S. A., Dominick, D., Mohd Nadzir, M. S., Sahani, M., and Tahir, N. M.: Seasonal effect and source apportionment of polycyclic aromatic hydrocarbons in $PM_{2.5}$, Atmos. Environ., 106, 178–190, doi:10.1016/j.atmosenv.2015.01.077, 2015b.

Khan, M. F., Latif, M. T., Lim, C. H., Amil, N., Jaafar, S. A., Dominick, D., Nadzir, M. S. M., Sahani, M., and Tahir, N. M.: Seasonal effect and source apportionment of polycyclic aromatic hydrocarbons in $PM_{2.5}$, Atmos. Environ., 106, 178–190, doi:10.1016/j.atmosenv.2015.01.077, 2015c.

Khanna, I., Khare, M., and Gargava, P.: Health Risks Associated with Heavy Metals in Fine Particulate Matter: A Case Study in Delhi City, India, J. Geosci. Environ. Protec., 3, 72–77, doi:10.4236/gep.2015.32012, 2015.

Kholdebarin, A., Biati, A., Moattar, F., and Shariat, S.: Outdoor PM_{10} source apportionment in metropolitan cities – a case study, Environ. Monit. Assess., 187, 1–12, doi:10.1007/s10661-015-4294-z, 2015.

Kim, E. and Hopke, P. K.: Source characterization of ambient fine particles in the Los Angeles basin, J. Environ. Eng. Sci., 6, 343–353, doi:10.1139/s06-054, 2007.

Kim Oanh, N. T., Upadhyay, N., Zhuang, Y. H., Hao, Z. P., Murthy, D. V. S., Lestari, P., Villarin, J. T., Chengchua, K., Co, H. X., Dung, N. T., and Lindgren, E. S.: Particulate air pollution in six Asian cities: Spatial and temporal distributions, and associated sources, Atmos. Environ., 40, 3367–3380, doi:10.1016/j.atmosenv.2006.01.050, 2006.

Kioumourtzoglou, M.-A., Coull, B. A., Dominici, F., Koutrakis, P., Schwartz, J., and Suh, H.: The impact of source contribution uncertainty on the effects of source-specific $PM_{2.5}$ on hospital admissions: A case study in Boston, MA, J. Expo. Sci. Env. Epid., 24, 365–371, doi:10.1038/jes.2014.7, 2014.

Lee, E., Chan, C. K., and Paatero, P.: Application of positive matrix factorization in source apportionment of particulate pollutants in Hong Kong, Atmos. Environ., 33, 3201–3212, doi:10.1016/S1352-2310(99)00113-2, 1999.

Lelieveld, J., Crutzen, P. J., Ramanathan, V., Andreae, M. O., Brenninkmeijer, C. A. M., Campos, T., Cass, G. R., Dickerson, R. R., Fischer, H., de Gouw, J. A., Hansel, A., Jefferson, A., Kley, D., de Laat, A. T. J., Lal, S., Lawrence, M. G., Lobert, J. M., Mayol-Bracero, O. L., Mitra, A. P., Novakov, T., Oltmans, S. J., Prather, K. A., Reiner, T., Rodhe, H., Scheeren, H. A., Sikka, D., and Williams, J.: The Indian Ocean Experiment: Widespread Air Pollution from South and Southeast Asia, Science, 291, 1031–1036, doi:10.1126/science.1057103, 2001.

Lestari, P. and Mauliadi, Y. D.: Source apportionment of particulate matter at urban mixed site in Indonesia using PMF, Atmos. Environ., 43, 1760–1770, doi:10.1016/j.atmosenv.2008.12.044, 2009.

Li, H., Wang, J., Wang, Q. G., Qian, X., Qian, Y., Yang, M., Li, F., Lu, H., and Wang, C.: Chemical fractionation of arsenic and heavy metals in fine particle matter and its implications for risk

assessment: A case study in Nanjing, China, Atmos. Environ., 103, 339–346, doi:10.1016/j.atmosenv.2014.12.065, 2015.

Li, Y., Zhang, Z., Liu, H., Zhou, H., Fan, Z., Lin, M., Wu, D., and Xia, B.: Characteristics, sources and health risk assessment of toxic heavy metals in $PM_{2.5}$ at a megacity of southwest China, Environ. Geochem. Health, in press, doi:10.1007/s10653-015-9722-z, 2015.

Maenhaut, W., Raes, N., Chi, X., Cafmeyer, J., and Wang, W.: Chemical composition and mass closure for $PM_{2.5}$ and PM_{10} aerosols at K-puszta, Hungary, in summer 2006, X-Ray Spectrom., 37, 193–197, doi:10.1002/xrs.1062, 2008.

Mariani, R. L. and de Mello, W. Z.: $PM_{2.5-10}$, $PM_{2.5}$ and associated water-soluble inorganic species at a coastal urban site in the metropolitan region of Rio de Janeiro, Atmos. Environ., 41, 2887–2892, doi:10.1016/j.atmosenv.2006.12.009, 2007.

Martins, V., Moreno, T., Minguillón, M. C., van Drooge, B. L., Reche, C., Amato, F., de Miguel, E., Capdevila, M., Centelles, S., and Querol, X.: Origin of inorganic and organic components of $PM_{2.5}$ in subway stations of Barcelona, Spain, Part A, Environ. Pollut., 208, 125–136, doi:10.1016/j.envpol.2015.07.004, 2016.

McGinnis, J. E., Heo, J., Olson, M. R., Rutter, A. P., and Schauer, J. J.: Understanding the sources and composition of the incremental excess of fine particles across multiple sampling locations in one air shed, J. Environ. Sci., 26, 818–826, doi:10.1016/S1001-0742(13)60508-2, 2014.

Meij, R. and te Winkel, H.: The emissions of heavy metals and persistent organic pollutants from modern coal-fired power stations, Atmos. Environ., 41, 9262–9272, doi:10.1016/j.atmosenv.2007.04.042, 2007.

Mohd Tahir, N., Suratman, S., Fong, F. T., Hamzah, M. S., and Latif, M. T.: Temporal distribution and chemical characterization of atmospheric particulate matter in the eastern coast of Peninsular Malaysia, Aerosol Air Qual. Res., 13, 584–595, doi:10.4209/aaqr.2012.08.0216, 2013.

Morales, R. and Leiva, G.: Distribution and Critical Concentration of PM in the city of Santiago, Chile (in Spanish), in: Atmospheric Urban Pollution: Critical episodes of the Environmental pollution in the City of Santiago, Chile (in Spanish), edited by: Morales, R. G. E., 1st edn., Editorial Universitaria SA, Santiago, Chile, 2006.

Moreno, T., Karanasiou, A., Amato, F., Lucarelli, F., Nava, S., Calzolai, G., Chiari, M., Coz, E., Artíñano, B., Lumbreras, J., Borge, R., Boldo, E., Linares, C., Alastuey, A., Querol, X., and Gibbons, W.: Daily and hourly sourcing of metallic and mineral dust in urban air contaminated by traffic and coal-burning emissions, Atmos. Environ., 68, 33–44, doi:10.1016/j.atmosenv.2012.11.037, 2013.

Mustaffa, N., Latif, M., Ali, M., and Khan, M.: Source apportionment of surfactants in marine aerosols at different locations along the Malacca Straits, Environ. Sci. Pollut. Res., 21, 6590–6602, doi:10.1007/s11356-014-2562-z, 2014.

Niu, L., Ye, H., Xu, C., Yao, Y., and Liu, W.: Highly time- and size-resolved fingerprint analysis and risk assessment of airborne elements in a megacity in the Yangtze River Delta, China, Chemosphere, 119, 112–121, doi:10.1016/j.chemosphere.2014.05.062, 2015.

Norris, G., Duvall, R., Brown, S., and Bai, S.: EPA positive matrix factorization (PMF) 5.0 fundamentals & user guide, Prepared for the US Environmental Protection Agency, Washington, DC, by the National Exposure Research Laboratory, Research Triangle Park, USA, 2014.

Ogulei, D., Hopke, P. K., and Wallace, L. A.: Analysis of indoor particle size distributions in an occupied townhouse using positive matrix factorization, Indoor Air, 16, 204–215, doi:10.1111/j.1600-0668.2006.00418.x, 2006a.

Ogulei, D., Hopke, P. K., Zhou, L., Patrick Pancras, J., Nair, N., and Ondov, J. M.: Source apportionment of Baltimore aerosol from combined size distribution and chemical composition data, Supplement 2, Atmos. Environ., 40, 396–410, doi:10.1016/j.atmosenv.2005.11.075, 2006b.

Paatero, P.: Least squares formulation of robust non-negative factor analysis, Chemometr. Intell. Lab., 37, 23–35, doi:10.1016/S0169-7439(96)00044-5, 1997.

Paatero, P. and Tapper, U.: Positive matrix factorization: A non-negative factor model with optimal utilization of error estimates of data values, Environmetrics, 5, 111–126, doi:10.1002/env.3170050203, 1994.

Pandey, P., Patel, D. K., Khan, A. H., Barman, S. C., Murthy, R. C., and Kisku, G. C.: Temporal distribution of fine particulates ($PM_{2.5}$, PM_{10}), potentially toxic metals, PAHs and Metal-bound carcinogenic risk in the population of Lucknow City, India, Part A, J. Environ. Sci. Health., 48, 730–745, doi:10.1080/10934529.2013.744613, 2013.

Polissar, A. V., Hopke, P. K., Malm, W. C., and Sisler, J. F.: Atmospheric aerosol over Alaska: 1. Spatial and seasonal variability, J. Geophys. Res., 103, 19035–19044, doi:10.1029/98JD01365, 1998a.

Polissar, A. V., Hopke, P. K., Paatero, P., Malm, W. C., and Sisler, J. F.: Atmospheric aerosol over Alaska: 2. Elemental composition and sources, J. Geophys. Res., 103, 19045–19057, doi:10.1029/98JD01212, 1998b.

Querol, X., Fernández-Turiel, J., and López-Soler, A.: Trace elements in coal and their behaviour during combustion in a large power station, Fuel, 74, 331–343, doi:10.1016/0016-2361(95)93464-O, 1995.

Rahman, S. A., Hamzah, M. S., Wood, A. K., Elias, M. S., Salim, A., Ashifa, N., and Sanuri, E.: Sources apportionment of fine and coarse aerosol in Klang Valley, Kuala Lumpur using positive matrix factorization, Atmos. Pollut. Res., 2, 197–206, doi:10.5094/APR.2011.025, 2011.

Reid, J. S., Hyer, E. J., Johnson, R. S., Holben, B. N., Yokelson, R. J., Zhang, J., Campbell, J. R., Christopher, S. A., Di Girolamo, L., Giglio, L., Holz, R. E., Kearney, C., Miettinen, J., Reid, E. A., Turk, F. J., Wang, J., Xian, P., Zhao, G., Balasubramanian, R., Chew, B. N., Janjai, S., Lagrosas, N., Lestari, P., Lin, N.-H., Mahmud, M., Nguyen, A. X., Norris, B., Oanh, N. T. K., Oo, M., Salinas, S. V., Welton, E. J., and Liew, S. C.: Observing and understanding the Southeast Asian aerosol system by remote sensing: An initial review and analysis for the Seven Southeast Asian Studies (7SEAS) program, Atmos. Res., 122, 403–468, doi:10.1016/j.atmosres.2012.06.005, 2013.

Remoundaki, E., Kassomenos, P., Mantas, E., Mihalopoulos, N., and Tsezos, M.: Composition and mass closure of $PM_{2.5}$ in urban environment (Athens, Greece), Aerosol Air Qual. Res., 13, 72–82, doi:10.4209/aaqr.2012.03.0054, 2013.

Sahani, M., Zainon, N. A., Mahiyuddin, W. R. W., Latif, M. T., Hod, R., Khan, M. F., Tahir, N. M., and Chan,

C.-C.: A case-crossover analysis of forest fire haze events and mortality in Malaysia, Atmos. Environ., 96, 257–265, doi:10.1016/j.atmosenv.2014.07.043, 2014.

Sánchez-Soberón, F., Rovira, J., Mari, M., Sierra, J., Nadal, M., Domingo, J. L., and Schuhmacher, M.: Main components and human health risks assessment of PM_{10}, $PM_{2.5}$, and PM_1 in two areas influenced by cement plants, Atmos. Environ., 120, 109–116, doi:10.1016/j.atmosenv.2015.08.020, 2015.

Santoso, M., Hopke, P. K., Hidayat, A., and Diah Dwiana, L.: Sources identification of the atmospheric aerosol at urban and suburban sites in Indonesia by positive matrix factorization, Sci. Total. Environ., 397, 229–237, doi:10.1016/j.scitotenv.2008.01.057, 2008.

Santoso, M., Lestiani, D. D., and Markwitz, A.: Characterization of airborne particulate matter collected at Jakarta roadside of an arterial road, J. Radioanal. Nucl. Chem., 297, 165–169, doi:10.1007/s10967-012-2350-5, 2013.

Satsangi, P. G., Yadav, S., Pipal, A. S., and Kumbhar, N.: Characteristics of trace metals in fine ($PM_{2.5}$) and inhalable (PM_{10}) particles and its health risk assessment along with in-silico approach in indoor environment of India, Atmos. Environ., 92, 384–393, doi:10.1016/j.atmosenv.2014.04.047, 2014.

Seinfeld, J. H. and Pandis, S. N.: Atmospheric chemistry and physics: from air pollution to climate change, John Wiley & Sons, New Jersey, USA, 2012.

Seneviratne, M., Waduge, V. A., Hadagiripathira, L., Sanjeewani, S., Attanayake, T., Jayaratne, N., and Hopke, P. K.: Characterization and source apportionment of particulate pollution in Colombo, Sri Lanka, Atmos. Pollut. Res., 2, 207–212, doi:10.5094/APR.2011.026, 2011.

Sillanpää, M., Hillamo, R., Saarikoski, S., Frey, A., Pennanen, A., Makkonen, U., Spolnik, Z., Van Grieken, R., Braniš, M., Brunekreef, B., Chalbot, M.-C., Kuhlbusch, T., Sunyer, J., Kerminen, V.-M., Kulmala, M., and Salonen, R. O.: Chemical composition and mass closure of particulate matter at six urban sites in Europe, Supplement 2, Atmos. Environ., 40, 212–223, doi:10.1016/j.atmosenv.2006.01.063, 2006.

Song, Y., Xie, S., Zhang, Y., Zeng, L., Salmon, L. G., and Zheng, M.: Source apportionment of $PM_{2.5}$ in Beijing using principal component analysis/absolute principal component scores and UNMIX, Sci. Total. Environ., 372, 278–286, doi:10.1016/j.scitotenv.2006.08.041, 2006.

Srimuruganandam, B. and Shiva Nagendra, S. M.: Application of positive matrix factorization in characterization of PM_{10} and $PM_{2.5}$ emission sources at urban roadside, Chemosphere, 88, 120–130, doi:10.1016/j.chemosphere.2012.02.083, 2012.

Streets, D., Yarber, K., Woo, J. H., and Carmichael, G.: Biomass burning in Asia: Annual and seasonal estimates and atmospheric emissions, Global Biogeochem. Cy., 17, 1099, doi:10.1029/2003GB002040, 2003.

Sun, Y., Zhuang, G., Tang, A., Wang, Y., and An, Z.: Chemical Characteristics of $PM_{2.5}$ and PM_{10} in Haze–Fog Episodes in Beijing, Environ. Sci. Technol., 40, 3148–3155, doi:10.1021/es051533g, 2006.

Taner, S., Pekey, B., and Pekey, H.: Fine particulate matter in the indoor air of barbeque restaurants: Elemental compositions, sources and health risks, Sci. Total. Environ., 454–455, 79–87, doi:10.1016/j.scitotenv.2013.03.018, 2013.

Tao, J., Zhang, L., Engling, G., Zhang, R., Yang, Y., Cao, J., Zhu, C., Wang, Q., and Luo, L.: Chemical composition of $PM_{2.5}$ in an urban environment in Chengdu, China: Importance of springtime dust storms and biomass burning, Atmos. Res., 122, 270–283, doi:10.1016/j.atmosres.2012.11.004, 2013.

Tao, J., Gao, J., Zhang, L., Zhang, R., Che, H., Zhang, Z., Lin, Z., Jing, J., Cao, J., and Hsu, S.-C.: $PM_{2.5}$ pollution in a megacity of southwest China: source apportionment and implication, Atmos. Chem. Phys., 14, 8679–8699, doi:10.5194/acp-14-8679-2014, 2014.

Taylor, S. R.: Abundance of chemical elements in the continental crust: a new table, Geochim. Cosmochim. Ac., 28, 1273–1285, 1964.

Terzi, E., Argyropoulos, G., Bougatioti, A., Mihalopoulos, N., Nikolaou, K., and Samara, C.: Chemical composition and mass closure of ambient PM_{10} at urban sites, Atmos. Environ., 44, 2231–2239, doi:10.1016/j.atmosenv.2010.02.019, 2010.

Thurston, G. D. and Spengler, J. D.: A quantitative assessment of source contributions to inhalable particulate matter pollution in metropolitan Boston, Atmos. Environ., 19, 9–25, doi:10.1016/0004-6981(85)90132-5, 1985.

Torfs, K. and Van Grieken, R.: Chemical relations between atmospheric aerosols, deposition and stone decay layers on historic buildings at the mediterranean coast, Atmos. Environ., 31, 2179–2192, doi:10.1016/S1352-2310(97)00038-1, 1997.

US EPA: Risk Assessment Guidance for Superfund, in: Part A: Human Health Evaluation Manual; Part E, Supplemental Guidance for Dermal Risk Assessment; Part F, Supplemental Guidance for Inhalation Risk Assessment, vol. I. available at: http://www.epa.gov/risk/risk-assessment-guidance-superfund-rags-part (last access: 28 August 2014), 2011.

Vedantham, R., Landis, M. S., Olson, D., and Pancras, J. P.: Source Identification of $PM_{2.5}$ in Steubenville, Ohio Using a Hybrid Method for Highly Time-Resolved Data, Environ. Sci. Technol., 48, 1718–1726, doi:10.1021/es402704n, 2014.

Vejahati, F., Xu, Z., and Gupta, R.: Trace elements in coal: Associations with coal and minerals and their behavior during coal utilization – A review, Fuel, 89, 904–911, doi:10.1016/j.fuel.2009.06.013, 2010.

Viana, M., Kuhlbusch, T. A. J., Querol, X., Alastuey, A., Harrison, R. M., Hopke, P. K., Winiwarter, W., Vallius, M., Szidat, S., Prévôt, A. S. H., Hueglin, C., Bloemen, H., Wåhlin, P., Vecchi, R., Miranda, A. I., Kasper-Giebl, A., Maenhaut, W., and Hitzenberger, R.: Source apportionment of particulate matter in Europe: A review of methods and results, J. Aerosol Sci., 39, 827–849, doi:10.1016/j.jaerosci.2008.05.007, 2008.

Wahid, N. B. A., Latif, M. T., and Suratman, S.: Composition and source apportionment of surfactants in atmospheric aerosols of urban and semi-urban areas in Malaysia, Chemosphere, 91, 1508–1516, doi:10.1016/j.chemosphere.2012.12.029, 2013.

Wåhlin, P., Berkowicz, R., and Palmgren, F.: Characterisation of traffic-generated particulate matter in Copenhagen, Atmos. Environ., 40, 2151–2159, doi:10.1016/j.atmosenv.2005.11.049, 2006.

Waked, A., Favez, O., Alleman, L. Y., Piot, C., Petit, J.-E., Delaunay, T., Verlinden, E., Golly, B., Besombes, J.-L., Jaffrezo, J.-L., and Leoz-Garziandia, E.: Source apportionment of PM_{10} in a north-western Europe regional urban background site (Lens, France) using positive matrix factorization and including pri-

mary biogenic emissions, Atmos. Chem. Phys., 14, 3325–3346, doi:10.5194/acp-14-3325-2014, 2014.

Wang, Y. and Hopke, P. K.: A ten-year source apportionment study of ambient fine particulate matter in San Jose, California, Atmos. Pollut. Res., 4, 398–404, doi:10.5094/APR.2013.045, 2013.

Watson, J. G., Robinson, N. F., Chow, J. C., Henry, R. C., Kim, B. M., Pace, T. G., Meyer, E. L., and Nguyen, Q.: The USEPA/DRI chemical mass balance receptor model, CMB 7.0, Environ. Softw., 5, 38–49, doi:10.1016/0266-9838(90)90015-X, 1990.

Wilson, T. R.: Salinity and the major elements of sea-water, in: Chemical Oceanography, edited by: Riley, J. P. and Skirrow, G., 365–413, Academic, San Diego, Calif., USA, 1975.

Wu, C.-F., Wu, S.-Y., Wu, Y.-H., Cullen, A. C., Larson, T. V., Williamson, J., and Liu, L. J. S.: Cancer risk assessment of selected hazardous air pollutants in Seattle, Environ. Int., 35, 516–522, doi:10.1016/j.envint.2008.09.009, 2009.

Wu, Y.-S., Fang, G.-C., Lee, W.-J., Lee, J.-F., Chang, C.-C., and Lee, C.-Z.: A review of atmospheric fine particulate matter and its associated trace metal pollutants in Asian countries during the period 1995–2005, J. Hazard. Mater., 143, 511–515, doi:10.1016/j.jhazmat.2006.09.066, 2007.

Yang, W., Zhang, S., Tang, J., Bu, K., Yang, J., and Chang, L.: A MODIS time series data based algorithm for mapping forest fire burned area, Chin. Geogr. Sci., 23, 344–352, doi:10.1007/s11769-013-0597-6, 2013.

Yin, J. and Harrison, R. M.: Pragmatic mass closure study for $PM_{1.0}$, $PM_{2.5}$ and PM_{10} at roadside, urban background and rural sites, Atmos. Environ., 42, 980–988, doi:10.1016/j.atmosenv.2007.10.005, 2008.

Yu, L., Wang, G., Zhang, R., Zhang, L., Song, Y., Wu, B., Li, X., An, K., and Chu, J.: Characterization and source apportionment of $PM_{2.5}$ in an urban environment in Beijing, Aerosol Air Qual. Res., 13, 574–583, 2013.

Zhang, H., Li, J., Ying, Q., Yu, J. Z., Wu, D., Cheng, Y., He, K., and Jiang, J.: Source apportionment of $PM_{2.5}$ nitrate and sulfate in China using a source-oriented chemical transport model, Atmos. Environ., 62, 228–242, doi:10.1016/j.atmosenv.2012.08.014, 2012.

Zhang, N., Han, B., He, F., Xu, J., Niu, C., Zhou, J., Kong, S., Bai, Z., and Xu, H.: Characterization, health risk of heavy metals, and source apportionment of atmospheric $PM_{2.5}$ to children in summer and winter: an exposure panel study in Tianjin, China, Air Qual. Atmos. Health, 8, 347–357, doi:10.1007/s11869-014-0289-0, 2014.

Zhang, R., Jing, J., Tao, J., Hsu, S.-C., Wang, G., Cao, J., Lee, C. S. L., Zhu, L., Chen, Z., Zhao, Y., and Shen, Z.: Chemical characterization and source apportionment of $PM_{2.5}$ in Beijing: seasonal perspective, Atmos. Chem. Phys., 13, 7053–7074, doi:10.5194/acp-13-7053-2013, 2013.

Zhang, X., Hecobian, A., Zheng, M., Frank, N. H., and Weber, R. J.: Biomass burning impact on $PM_{2.5}$ over the southeastern US during 2007: integrating chemically speciated FRM filter measurements, MODIS fire counts and PMF analysis, Atmos. Chem. Phys., 10, 6839–6853, doi:10.5194/acp-10-6839-2010, 2010.

Zhang, Z., Gao, J., Engling, G., Tao, J., Chai, F., Zhang, L., Zhang, R., Sang, X., Chan, C.-Y., Lin, Z., and Cao, J.: Characteristics and applications of size-segregated biomass burning tracers in China's Pearl River Delta region, Atmos. Environ., 102, 290–301, doi:10.1016/j.atmosenv.2014.12.009, 2015.